Photoluminescence Studies of Eu^{3+} and Zn^{2+} Codoped $CaNb_2O_6$ phosphors for Solid State Lighting Applications

A dissertation submitted in

partial fulfillment of the requirement for the award of the degree

of

Master of Technology

in

Nanoscience and Technology

by

MUDIT BANSAL
2K10/NST/08

Under the supervision of

Dr. M. JAYASIMHADRI
Assistant Professor
Department of Applied Physics

Submitted to

Department of Applied Physics
Delhi Technological University

(Formerly Delhi College of Engineering)
Main Bawana Road, Shahabad, Daulatpur, Delhi-110042

June 2012

Contents

Certificate **i**

Acknowledgements **ii**

Abstract **iii**

1. Introduction **Page No.**

1.1 History 2

1.2 Importance of rare-earths 3

1.3 Introduction to luminescence 5

1.4 Phosphor and luminescence mechanisms 9

1.5 Applications 13

1.6 **Motivation** 17

1.7 Aim of the thesis 18

References 19

2. Characterization techniques and sample preparation **20**

2.1 X-ray diffraction 21

2.2 Scanning electron microscope 23

2.3 Photoluminescence 26

2.4 TGA-DSC 29

2.5 Sample preparation 32

References 34

3. Results and discussions **35**

3.1 TGA-DSC analysis 36

3.2 XRD 37

3.3 SEM 38

3.4 Excitation spectra 39

3.5 Emission spectra 40

3.6 Chromaticity coordinates 46

References 49

Department of Applied Physics

Delhi Technological University

Delhi

CERTIFICATE

This is to certify that the dissertation entitled "Photoluminescence studies of Eu^{3+} and Zn^{2+} codoped $CaNb_2O_6$ phosphors for solid state lighting applications" submitted by Mr. Mudit Bansal in the partial fulfillment of the requirement for the award of the degree of M.Tech. in Nanoscience and Technology from the Department of Physics, Delhi Technological University, Delhi is a record of candidate's own work carried out by him under my supervision. The matter embodied in this report has not been submitted in the part or full to any other university or institute for the award of any degree.

Dr. M. Jayasimhadri

HOD
Applied Physics Department
Delhi Technological University
Delhi-110042

ACKNOWLEDGEMENTS

It is a pleasure to present my thesis on "Photoluminescence studies of Eu^{3+} and Zn^{2+} codoped $CaNb_2O_6$ phosphors for solid state lighting applications" under the inspiring direction and supervision of my Professor **Dr. M. JAYASIMHADRI,** who gave me constant encouragement and ample time for the completion of this research without which this Thesis would have been far from complete.

It gives me immense pleasure to express my heartfelt thanks **Prof. R.K. Sinha,** Head, Department of Physics, and for providing me the necessary facilities to carry out the research work.

I would like to express my heartfelt thanks to **Dr. D. Harnath, Mr. Bathula Sivaiah**, National Physical Laboratory, New Delhi, for their help in measuring the PL, XRD, TG-DTA in their laboratory.

I am also thankful to **Mr. Amit Kumar Viswakarma**, Ph.D. student in Luminescent Materials Research Lab, for his timely help during my M.Tech. course.

I am also thankful to my friend **Kamal Singh**, M.tech student, Nanoscience and Technology for providing me well-timed access in furnishing required research papers.

I express my expanse gratitude to **my father Mr. Rajinder Kumar Bansal and my mother Mrs. Rashmi Bansal** for their indefatigable support in helping me to not only complete the dissertation but standing erect face to face against my troubles and abruptly fulfilling all my impulsive decisions during my whole M.Tech. dissertation work without which timely submission of this dissertation would be improbable and therefore, I dedicate this thesis to my loving parents.

I greatly acknowledge the authorities of **Delhi Technological University, Delhi** for providing me all the necessary facilities. I am highly indebted to DAE-BRNS**,** BARC, Mumbai for providing the financial assistance to procure chemicals related to this research.

Mudit Bansal

Masters of Technology

Nanoscience and Technology

Roll No. 08/NST/2010

Abstract

A novel phosphor $Ca_{0.9-x}Zn_{0.1}Nb_2O_6$: Eu_x prepared by using solid state reaction at 1050 ^oC. The photoluminescence properties are investigated in which the excitation spectrum exhibited a charge transfer band in the UV region centered at 266 nm and a sharp peak corresponding to $^7F_0$-$^5L_6$ at 395 nm. Emission properties also measured for these niobate phosphors under the 266 and 395 excitation. A broad emission band and 4f-4f transitions of Eu^{3+} were observed by exciting at 266 nm. By exciting the samples at 266 nm leads to energy transfer from the excited state of $[NbO_6]^{7-}$ to the $^5D_0$ band of Eu^{3+} via the down-converting energy transfer process. The effect of energy transfer on the emission bands was explained under the excitation 266 nm. The concentration dependence emission properties were measured and the results indicate that the emission intensity increases with Eu^{3+} concentration up to 2.5 mol%, beyond that concentration the emission intensity decreases due to concentration quenching. The intense peak observed in both the cases could be attributed to $^5D_0$-$^7F_2$ transition in Eu^{3+} ions. In order to evaluate the colorimetric performance of the phosphor, the CIE coordinates for the calcium niobate phosphors were calculated using the emission spectra excited by 266 nm and 395 nm. These results show that blue light emitted for undoped sample and tunable color in the white region and finally red can be obtained by adjusting the Eu^{3+} concentration. Moreover, the chromaticity coordinates of these phosphors under the excitation of 266 nm are located in the boundary of white-light region. Due to the flexibility of colour tuning of this phosphor, this host will be potential candidate to use in solid state lighting applications.

CHAPTER 1

Introduction

1.1 History

The word *phosphor* was invented in the early of 17th century and an alchemist, Vincentinus Casciarolo of Bologna, Italy, found a heavy crystalline stone with a gloss at the foot of a volcano, and fired it in a charcoal oven intending to convert it to a noble metal. But instead of metal, he found that the sintered stone emitted red light in the dark after exposure to sunlight. This stone was called the "Bolognian stone", which is shown in Figure 1.1. This stone is now known as barite ($BaSO_4$), with the fired product being BaS, which is now known to be a host for phosphor materials.

Figure 1.1: Bolognian stone

Phosphor means "light bearer" in Greek, and appears in Greek myths as the personification of the morning star Venus. The word *phosphorescence*, which means persisting light emission from a substance after the exciting radiation has ceased, was derived from the word *phosphor*.

Prior to the discovery of Bolognian stone, the Japanese were reported to have prepared phosphorescent paint from seashells. This fact is described in a 10th century Chinese document.

Presently, the word *luminescence* is defined as a phenomenon in which the electronic state of a substance is excited by some kind of external energy and the excitation energy is given off as light.

the inorganic *phosphors*, usually those in powder form and synthesized for the purpose of practical applications. The word phosphor is equivalent to "solid luminescent material". Single crystals, thin films, and organic molecules that exhibit luminescence are rarely called phosphors.[6]

1.2 Importance of Rare-earths

Of all the groups in the periodic table of chemical elements perhaps the most fascinating are those commonly known as the rare earth elements or the lanthanide series. The lanthanides from a special group of elements, usually shown at the bottom of the periodic table. 4f block elements are also called as lanthanides, lanthanons or rare earths. The first two names are given because of their strong resemblance to lanthanum. The name rare earth was given to them because they were originally extracted from oxides for which ancient name was earth and which were considered to be rare. In fact the name lanthanides has been derived from lanthanum, which is the prototype of lanthanides. Lanthanides constitute the first inner transition series. Furthermore, the group of elements known as lanthanide comprises fifteen elements in which a progressive filling of the 4f shell occurs. The group starts with lanthanum (Z=57) and ends with lutetium (Z=71). Table 1.1 gives the electronic configuration of lanthanide ions along with their ground states.

The history of the lanthanides started in 1788, when captain Arrhenius found a black stone near Yetterby in Sweden. In lanthanide group, the ions differ in the number of electrons in the 4f shell. The ground state electronic configuration is $4f^N$ and the first excited configuration is $4f^{N-1}5d$. The RE ions in solids exist either in divalent or trivalent. Their electronic configuration is $4f^N\ 5s^2\ 5p^6$ or $4f^{N-1}5s^2\ 5p^6$, respectively. By far the most common valence state of the RE ions in solids is the trivalent one. The electron configuration of tripositive rare earth ions are presented in Table 1.1. The 4f electrons are not the outer most ones. The 4f orbitals are shielded from the surrounding by the filled $5s^2\ 5p^6$ orbitals, which explains the "atomic" nature of their spectra. Thus the 4f electrons are only weakly perturbed by the charge of the surrounding ligands. The spectra of Ln compounds are sharp and are similar to the spectra of atoms. The shielded character of the 4f orbitals is also responsible for the unique optical properties of rare earth ions. By the early, 1960's the Johns Hopkins group, under the direction of Dieke had generated complete set of energy level assignments for all trivalent rare earth ions in anhydrous trichlorides. It is useful as a good guide for the location of J states of the trivalent rare earths, since the centers of gravity of J manifolds exhibit very small variations with the host. The order and separation of the levels within a J manifold on the other hand, vary considerably from host to host. The overall extent of the crystalline Stark splittings is small on the energy scale.

Table 1.1

The electronic configurations of rare earth (RE) ions with their ground state terms

Atomic number (Z)	Lanthanide Element	Symbol	Neutral Atom Electronic configuration	Trivalent atom (RE^{3+})	
				Electronic configuration	Ground term
57	Lanthanum	La	[Xe] $4f^0\ 5d^1\ 6s^2$	[Xe] $4f^0$	$^1S_0$
58	Cerium	Ce	[Xe] $4f^2\ 6s^2$	[Xe] $4f^1$	$^2F_{5/2}$
59	Praseodymium	Pr	[Xe] $4f^3\ 6s^2$	[Xe] $4f^2$	$^3H_4$
60	Neodymium	Nd	[Xe] $4f^4\ 6s^2$	[Xe] $4f^3$	$^4I_{9/2}$
61	Promethium	Pm	[Xe] $4f^5\ 6s^2$	[Xe] $4f^4$	$^5I_4$
62	Samarium	Sm	[Xe] $4f^6\ 6s^2$	[Xe] $4f^5$	$^6H_{5/2}$
63	Europium	Eu	[Xe] $4f^7\ 6s^2$	[Xe] $4f^6$	$^7F_0$
64	Gadolinium	Gd	[Xe] $4f^7\ 5d^1\ 6s^2$	[Xe] $4f^7$	$^8S_{7/2}$
65	Terbium	Tb	[Xe] $4f^9\ 6s^2$	[Xe] $4f^8$	$^7F_6$
66	Dysprosium	Dy	[Xe] $4f^{10}\ 6s^2$	[Xe] $4f^9$	$^6H_{15/2}$
67	Holmium	Ho	[Xe] $4f^{11}\ 6s^2$	[Xe] $4f^{10}$	$^5I_8$
68	Erbium	Er	[Xe] $4f^{12}\ 6s^2$	[Xe] $4f^{11}$	$^4I_{15/2}$
69	Thulium	Tm	[Xe] $4f^{13}\ 6s^2$	[Xe] $4f^{12}$	$^3H_6$
70	Ytterbium	Yb	[Xe] $4f^{14}\ 6s^2$	[Xe] $4f^{13}$	$^2F_{7/2}$
71	Lutetium	Lu	[Xe] $4f^{14}\ 5d^1\ 6s^2$	[Xe] $4f^{14}$	$^1S_0$

Trivalent lanthanides have been the most extensively used as activator ions because of the following reasons:

(i) They emit narrow lines, almost monochromatic light and have long emission lifetimes.

(ii) They possess many fluorescing states and wavelengths to choose among the 4f electronic configurations

(iii) Their intraconfigurational f-f transitions have small homogeneous line widths.

(iv) The local fields in phosphors can be treated as small perturbations on the free-ion energy levels.

1.3 Introduction to luminescence

Luminescence is defined as the radiation emitted by a molecule, or an atom, after it had absorbed energy to go to an excited state.

1.3.1 Fluorescence

A luminescence is a phenomenon in which electron de-excitation occurs almost spontaneously, and in which emission from a luminescent substance ceases when the exciting source is removed. If A^* denotes an excited state of a substance *A*, then fluorescence consists of the emission of a photon, [8]

$$A^* \rightarrow A + h\nu,$$

Once a molecule arrives at the lowest vibrational level of an excited singlet state, the molecule undergoes several processes, one of which is to return to the ground state by photon emission. This process is called *fluorescence*. The lifetime of an excited singlet state is approximately 10^{-9} to 10^{-7} sec and therefore the decay time of fluorescence is of the same order of magnitude. If fluorescence is unperturbed by competing processes, the lifetime of fluorescence is the intrinsic lifetime of the excited singlet state.

1.3.2 Phosphorescence is a specific type of photoluminescence related to fluorescence. Unlike fluorescence, a phosphorescent material does not immediately re-emit the radiation it absorbs. The slower time scales of the re-emission are associated with "forbidden" energy state transitions in quantum mechanics. As these transitions occur less often in certain materials, absorbed radiation may be re-emitted at a lower intensity for up to several hours. A delayed luminescence is a luminescence that persists even after removal of the exciting source. It is sometimes called afterglow**.**[9]

Figure. 1.2 Phosphorescence

1.3.3. Types of Luminescence

Bioluminescence, i.e. luminescence generated by a living organism

The light generating molecules become excited by a chemical reaction; bioluminescence is thus related to *chemiluminescence*. Some biological entities like bugs, e.g. ***fireflies***, denizens of the deep like anglerfish, some mushrooms and even bacteria can control this reaction. They produce the chemicals *luciferin* (a pigment) and *luciferase* (an enzyme). The luciferin reacts with oxygen to create light. The luciferase acts as a catalyst to speed up the reaction.

Chemiluminescence (or "chemoluminescence") results from some (actually amazingly few) chemical or electrochemical reactions

The energy needed comes from the reaction enthalpy. The reaction produces some new molecule that can have its electrons in an excited state right after it was formed. Decay to a ground state may then produce visible light. The flash of light one see when some dynamite explodes is not chemiluminescence even so the energy comes from a chemical reaction but simply black body radiation or **incandescence** from things getting very hot very quickly.

Crystalloluminescence is occasionally produced during crystallization. It is another variant of chemiluminescence because the energy comes essentially from bonding between atoms.

Electroluminescence generates light in response to an electric current passing through some material

In essence, electroluminescence results radiative recombination of electrons and holes; typically (but not exclusively) in semiconductors. It is the basis for LED's and semiconductor Lasers are thus of prime importance in the context of light sources.

Recently electroluminescence is also used for characterizing solar cell. Feed a large current into a *good* solar cell in the dark and IR camera will see (weak) electroluminescence even so **Si** is an indirect semiconductor. The reason is simple: Good solar cells, by definition, are **Si** devices where all regular recombination channels have been "closed off", i.e. made inefficient, otherwise the solar cell cannot be good. Radiant recombination then "wins" and is raised to a level where it can be detected.

Cathodoluminescence occurs when an electron beam impacts on a luminescent material such as a "phosphor"

For almost 100 years cathodoluminescence was used for making displays, classical *cathode* ***ray tube*** or TV tube that was recently replaced by flat screen displays like LCD's.

We still need cathodoluminescence for electron microscope (*TEM* type) screens for obvious reasons. But we can also look at the cathodoluminescence that specimen produce in the electron beam of an *SEM*; then we use it as an analytical tool. The "phosphors" tend to be

large bandgap semiconductors line **ZnO**, if color is needed like for an (old fashioned) TV, more involved different materials emitting red, green, and blue are necessary.

Mechanoluminescence, resulting from any mechanical action on a solid, can be subdivided into:

Triboluminescence . It happens when bonds in a material are broken because that material is scratched, crushed, or rubbed. The effect is not really understood; separation and reunification of electrical charges seems to play a role; and there might simply be sparking in large electric fields.

Fractoluminescence, same as triboluminescence.

Piezoluminescence, is produced by the action of pressure on piezoelectric materials.

Photoluminescence is caused by moving electrons to energetically higher levels through the absorption of photons.

It is easily done in semiconductors with photons of energy larger than the bandgap, radiating recombination channels that produce bandgap light. It was irradiated with very intense red light; the luminescence occurs in the IR.

Radioluminescence is generated when some materials are exposed to ionizing radiation. It was used, even so that is hard to believe nowadays, to make watch dials glow in the around 1960. A mixture of radium and copper-doped zinc sulfide was used to paint the dials, giving a greenish glow.

It is used for detecting ionizing radiation, especially x rays, by analyzing the light flashed generated when a quant is absorbed in certain crystals.

Sonoluminescence is the emission of short bursts of light from imploding bubbles in a liquid when excited by sound.

It had been known for some time but produced a lot of excitement in 1989 when stable single-bubbles could be produced that emit intense light in very short bursts. The mechanism is not really clear at present and rather outlandish explanations (e.g. an analogy to radiation

from black holes or nuclear fusion taking place)) have been proposed by well known scientists. It appears likely, however, that the bubbles "just" produce extremely hot plasma (up to 20.000 K) for very short times.

Thermoluminescence, describes the phenomenon that certain crystalline materials emit light when heated that is *not* black body radiation or incandescence

In this the previously absorbed energy from, e.g., electromagnetic or ionizing radiation was stored (meaning the excited electrons just stay on upper energy levels), typically at defects. It is released in the form of light if some thermal energy allows the excited electrons to overcome the energy barrier that kept then "up".

Thermoluminescence is an important method for dating some archeological artifacts. Ceramic parts being buried receive some ionizing dose from radioactive elements in the soil or from cosmic rays that is proportional to their age - and so is the intensity of the luminescence produced upon heating [11].

1.4 PHOSPHORS AND LUMINESCENT MECHANISMS

Phosphors, are mostly solid inorganic materials consisting of a host lattice, usually intentionally doped with rare-earth impurities and are capable of converting the absorbed energies into visible light. The impurity concentrations generally are low in view of the fact that at higher concentrations the efficiency of the luminescence process usually decreases due to the concentration quenching and energy transfer processess. When phosphors are illuminated by UV light, electrons are excited to higher energy level and energy is transferred to activator ions that are responsible for the visible light emission after returning to the ground state. Especially for fluorescent lamps, this is an essential feature to prevent absorption of visible light by the phosphors used. The absorption of energy, which is used to excite the luminescence, takes place by either the host lattice or by intentionally doped impurities. In most cases, the emission takes place due the

Figure 1.3 Phosphor powders

impurity ions, also called activator ions. When the activator ions show too weak an absorption, a second kind of impurities can be added (sensitizers), which absorb the energy and subsequently transfer the energy to the activators. This process involves transport of energy through the luminescent materials.

Quite frequently, the emission color can be adjusted by choosing the proper impurity ion, without changing the host lattice in which the impurity ions are incorporated. On the other hand, quite a few activator ions show emission spectra with emission at spectral positions which are hardly influenced by their chemical environment. This is especially true for many of the rare-earth ions.

1.4.1 Excitation Mechanisms

1.4.1.1 Optical Excitation of Luminescence and Energy Transfer

When absorption of UV or even visible light leads to emission, one speaks of optical excitation of luminescence. This process takes place in, e.g., fluorescent lamps and phosphor-converted LEDs, in which phosphors are used to at least partly change the wavelength of the radiation emitted by the LED. Optical absorption can take place on the already discussed impurities (optical centers), being either the activator ions or the sensitizer ions. Sensitizer ions are used when the optical absorption of the activator ions is too weak (e.g., because the optical transition is forbidden) to be useful in practical devices. In such a case, energy transfer from the sensitizer ions to the activator ions has to take place. The optical absorption leading to emission can also take place by the host lattice itself (band absorption). In this case one speaks of host lattice sensitization. Energy transfer from host lattice states to the activator ions (in some cases also involving sensitizers) has to take place.

1.4.1.2 Energy Transfer Mechanisms between Optical Centers

Energy transfer between a sensitizer ion (S) and an activator ion (A) can be written as a chemical reaction:

$$S^* + A - A^* + S$$

Where, the asterisk indicates the excited state.

1.4.1.3 Mechanisms Underlying Energy Transfer

For energy transfer, the sensitizer ion and the activator ion have to show physical interaction. This energy transfer can find its origin in electrostatic and exchange interaction. In addition, the emission spectrum of the sensitizer ion and the absorption spectrum of the activator ion have to show spectral overlap, for energy conservation reasons.

1.4.1.4 Cross-relaxation and Energy Transfer

In such a process, which can also be looked upon as energy transfer, the excited ion transfers only part of its energy to another ion. For two Tb^{3+} ions, the energy difference between the $^5D_3$ and $^5D_4$ excited states matches approximately the energy difference between the $^7F_6$ ground state and higher ^7F_J states. As in the energy transfer processes discussed above, at large Tb-Tb distances, the process of cross-relaxation has a low rate. In many host lattices, therefore, at low Tb concentration, emission from both the $^5D_3$ and $^5D_4$ excited states is observed (unless the gap between these two states is bridged by phonon emission, for which relatively high-energy phonons are required, which is, for example, the case with $InBO_3$: Tb). The resulting emission spectrum has emission from the near UV into the red part of the optical spectrum. At higher Tb concentrations (in the order of five percent), cross relaxation quenches the emission from the $^5D_3$ level in favor of emission originating from the $^5D_4$ level, implying that it is not possible to obtain blue Tb^{3+} emission in luminescent materials with higher Tb^{3+} concentrations. Cross-relaxation also occurs for other ions. It quenches blue Eu^{3+} emission even at relatively low Eu^{3+} concentrations (<1 %) in favor of the well-known red emission. In case of ions like Sm^{3+} and Dy^{3+}, cross-relaxation leads to quenching of the visible emission. This seriously limits the applicability of these ions.

1.4.1.5 Factors Determining the Emission Color

Many luminescent ions show emission at different wavelengths in different host lattices. This phenomenon, once understood, opens up the possibility to change, within certain limits, the emission color. In this way, the emission spectra (and excitation spectra) can be tuned toward the specifications required.

In cases where at least one of the electronic states is involved in the chemical bonding, the coupling to the lattice has to be taken into account. This situation is encountered for many transition metal ions, for the s^2 ions, and for rare-earth ion showing d-f emission.

Other rare-earth ions showing d-f emission are Ce^{3+}, Pr^{3+}, Nd^{3+} and Er^{3+}, albeit for the last three ions only in the UV.

The energy difference between the d- and f-electrons is modified by the covalence of the Eu^{2+}-ligand bond and the crystal field strength. An increase of the covalence of the Eu^{2+}-ligand bond results in a lower energy difference of the 4f-5d energy separation (due to the nephelauxetic effect). This elementary treatment considers the shift of the center of gravity (also called barycenter) of the d-electron level (also called centroid shift), i.e. any splitting is not yet taken into account. The crystal field interaction splits the d-level, depending on symmetry and crystal field strength. In this way, e.g., for Eu^{2+}, emission can be obtained extending from the UV part of the optical spectrum (where even line emission is possible) to the red part. Both are easily accessible by choosing appropriate host lattices, and for this reason broad-band emitters can in general be tuned within a large spectral range and can be adapted to the application needs. The spectral position of the emission lines due to transitions between f-electronic states does not vary very much on changing the host lattice. However, the relative emission intensity of the several possible optical transitions does vary considerably. It is stated that in cases where the rare-earth ion occupies a site with inversion symmetry, the selection rule states: $\Delta J=0, 1$. In cases where $\Delta J=0$, any transition to another state with $J=0$ is forbidden as well. In such a case, $\Delta|J|$ is necessarily +1. These are all magnetic dipole transitions. In lattices without inversion symmetry there is also electric dipole emission. For these transitions, the selection rule is: $\Delta|J|<=6$. Here again, for initial or final states with $J=0$, other selection rules are operative. In such a case, for electric dipole transitions, $\Delta|J|=2, 4$, or 6. We observe that the presence of an inversion center opens up the possibility to tune the emission spectrum to a small extent. For Eu^{3+} with excited state $^5D_0$, the emission can be tuned from orange (590 nm, with inversion symmetry, $^5D_0$-$^7F_1$ transition) to red (610 nm, without inversion symmetry, $^5D_0$-$^7F_2$ transition). More generally, these effects can be described by the Judd-Ofelt theory. As a function of three parameters, all possible spectra can be calculated. However, a direct coupling to the chemical environment is lacking. Nevertheless, such calculations are useful. Apart from being able to calculate the relative intensities, these calculations can also be used to calculate subsequent optical transitions, i.e. quantum cutters. For Pr^{3+}, in principle a quantum efficiency of 198%can be obtained in the visible. The same kind of calculation has shown that for Tm^{3+}, no quantum cutter, a yield of two visible photons can be obtained. Finally, in the case of donor-acceptor pair luminescence,

both the donors and the acceptors and the magnitude of the band gap strongly influence the spectral position of the emission color to be obtained. ZnS:Ag and ZnS:Cu.

As argued above, in general, the luminescent materials applied operate at physical limits in terms of absorption of the exciting radiation and the quantum efficiency (number of visible photons generated divided by the number of photons absorbed) with which luminescence is generated. In cathode ray tubes, the energy efficiency of the phosphors used is at maximum (up to about 25 %, see above), and the quantum efficiency of the luminescent centers is almost 100 %.

In plasma display panels, fluorescent lamps, and LEDs, the quantum efficiency amounts about 100 %, and the absorption coefficient is also very high. Nevertheless, the energy efficiency of luminescent devices is rather low in which the energy loss in factorized. The phosphor energy loss factor in this table is mainly determined by the Stokes shift (the difference in photon energy of radiation absorbed and emitted). This results in energy loss, which can be significant even when the quantum efficiency is 100 %.

1.4.1.6 Luminescence Quantum Yield and Quenching Processes

In this section, energy loss processes are discussed to throw some light on the question why all phosphors do not have a quantum efficiency of unity and what the loss processes are and also degradation processes in luminescent materials, which quite frequently occur during the operation of devices utilizing phosphors and which have a negative effect on the performance of such devices.

1.5 Applications

1.5.1 Lighting

Phosphor layers provide most of the light produced by fluorescent lamps, and are also used to improve the balance of light produced by metal halide lamps. Various neon signs use phosphor layers to produce different colors of light. Electroluminescent displays found, for example, in aircraft instrument panels, use a phosphor layer to produce glare-free illumination or as numeric and graphic display devices.

1.5.2 Phosphor Thermometry

Phosphor thermometry is a temperature measurement approach that uses the temperature dependence of certain phosphors for this purpose. For this, a phosphor coating is applied to a surface of interest and, usually, the decay time is the emission parameter that indicates temperature. Because the illumination and detection optics can be situated remotely, the method may be used for moving surfaces such as high speed motor surfaces. Also, phosphor may be applied to the end of an optical fiber as an optical analog of a thermocouple.

1.5.3 Cathode Ray Tubes

Various phosphors are available depending upon the needs of the measurement or display application. The brightness, color, and persistence of the illumination depend upon the type of phosphor used on the CRT screen. Phosphors are available with persistence ranging from less than one microsecond to several seconds. For visual observation of brief transient events, a long persistence phosphor may be desirable. For events which are fast and repetitive, or high frequency, a short-persistence phosphor is generally preferable.

A CRT has a vacuum tube containing an electron gun cathode and a phosphor coated screen. The cathode is a source of the electron beam and electrons generated into the vacuum are attracted by an anode. The electrons are then focussed and accelerated toward the screen by focussing and accelerating anode. Copper windings are wrapped around the tube and they act as steering coils. These coils create magnetic fields inside the tube and these magnetic fields steers the beam toward the screen. By varying the voltages in these coils, the electron beam can be positioned at any point on the screen. When the electron beam strikes the phosphor coated screen, a tiny bright visible spot is created on the screen. An image is formed when the beam is rastered across the screen. Colour CRTs have three electron guns, one for each primary colour. CRTs are used in oscilloscopes, television and computer monitors and radar targets. Typical values of cathode to anode distance range between 25 to 100 cm. CRTs are very bulky and when bigger screens are required the length of the tube must increase.

1.5.4 Phosphor in luminescent paints and printing ink

Long persistence phosphor can be mixed with various transparent resins, such as acrylic acid resin, polyurethane, epoxy, amino, polyvinyl butyral, and polyamide resin, becoming luminous paint and printing ink. The recommended percentage of long persistence phosphor in paint is about 10 - 50%, however, 30 - 60% in printing ink. First, these resins should be dissolved with some appropriate solvents into a solution, then long persistence phosphor will be added into the solution. Some anti-precipitating agents, ridding foaming agents and dispersing agents also need to be added into the solution, well mixed into a uniform solution by using a high speed mixer. However it must be avoided to grind them with mechanic abrader in order to keep the property of the pigment. In the case to use sand abrader becomes necessary, the grinding time should be as short as possible.[12]

1.5.5 Field emission displays

A **field emission display** (**FED**) is a display technology that incorporates flat panel display technology that uses large-area field electron emission sources to provide electrons that strike colored phosphor to produce a color image as a electronic visual display. In a general sense, a FED consists of a matrix of cathode ray tubes, each tube producing a single sub-pixel, grouped in threes to form red-green-blue (RGB) pixels. FEDs combine the advantages of CRTs, namely their high contrast levels and very fast response times, with the packaging advantages of LCD and other flat panel technologies. They also offer the possibility of requiring less power, about half that of an LCD system.[13]

1.5.5 Biological Labelling

The use of labelling or staining agents has greatly assisted the study of complex biological interactions in the field of biology. In particular, fluorescent labelling of biomolecules has been demonstrated as an indispensable tool in many biological studies. Types of fluorescent labelling agents that are commonly used include conventional classes of organic fluorophores such as fluorescein and cyanine dyes, as well as newer types of inorganic nanoparticles such as QDs, and novel fluorescent latex/silica nanobeads.

1.5.6 X-ray and scintillators

Intensifying screens are made of highly sensitive phosphors and used with photofluorography. When we are X-rayed, they reduce irradiation to one hundredth of the ordinal irradiation without intensifying screens.

- Our intensifying screens have high sensitivity and high sharpness by our technology that makes a high-density phosphor layer and prepares optimal grain size distribution.
- Sensitivity and sharpness are further improved by our structural designing that ensures effective light reflection and X-ray absorption characteristics.
- The surfaces of intensifying screens are protected with a special film to prevent darts and scars and to render handling easy.[14]

1.6 Motivation

Recently growing interest is focused on phosphor converted white light emitting diodes (pc-WLEDs), which have many advantages in comparison with incandescent and fluorescent lamps, such as higher efficiency, lack of toxic mercury, longer lifetime, lower power consumption and environment-friendly characteristics [1,2]. The common approach for manufacturing white LEDs is to use a yellow-emitting $(Y,Gd)_3(Al,Ga)_5O_{12}:Ce^{3+}$ ($YAG:Ce^{3+}$) phosphor with a blue InGaN LED chip. However, these white LEDs have some problems, such as low color rendering index, low color reproducibility, halo effect and low luminous efficiency. Furthermore, the color temperature is too high (6000-7000K) to be applied as an indoor warm lighting because of the lack of red light component [3]. Another strategy to obtain white LEDs is by pumping red, green and blue tricolor phosphors with a near-UV InGaN chip giving relatively high CRI values and also chromaticity coordinates remains constant during forward bias current increase. The common phosphors for the near-UV excitation are $Y_2O_2S:Eu^{3+}$ for red, $ZnS(Cu^{2+},Al^{3+})$ for green, and $BaMgAl_{10}O_{17}:Eu^{2+}$ (BAM) for blue[5]. Among these phosphors, $Y_2O_2S:Eu^{3+}$ shows lower efficiency compared with that of the blue and green phosphors, and chemical instability due to release of sulfide gas [4]. In addition, the lifetime of the $Y_2O_2S:Eu^{3+}$ material is inadequate under extended UV irradiation. Thus it is important to search for new red phosphors with high efficiency, high color purity, chemical stability, no environmental hazards and high absorption within near UV to blue region. Therefore the excitation peak at 395 nm is of immense importance in preparing novel phosphors, which motivated us to prepare Eu^{3+} and Zn^{2+} $CaNb_2O_6$ phosphors

It has been proposed in the literature that d electrons in an M^{2+} ion of MNb_2O_6, such as Zn, favor the delocalization of the electrons belonging to the niobate group relative to that of Ca^{2+}. Zn (0.74 A°) is actually smaller in size than Ca (0.99 A°) and based on the purely electrostatic interactions it would appear initially that its substitution would cause a contraction in the lattice leading to a decrease in the crystal field experienced by the luminescent center and hence a reduction in the intensity of the emission. However, Zn^{2+} (a transition metal ion) has a different chemical nature than the alkali earth metals and its delocalized d electrons might be able to participate in the O^{2-} to Nb^{5+} charge transfer, which would enhance the luminescence intensity. It is known that the Zn end member exhibits a blue luminescence under 254 nm that is very weak and is also included in the alloy system. It was observed that the largest increase in intensity due to Zn substitution was for

10% Zn addition. [7].

About the host (Calcium Niobate) :

Calcium niobate which has an orthorhombic crystal structure belongs to the family of columbite structural compounds and has a high refractive index varying from 2.07 to 2.20 and a specific gravity of 4.80g/cm. They have been studied as microwave dielectric materials, holographic applications and laser medias. $CaNb_2O_6$ possess a low symmetry crystal structure and distorted substitutional sites. In the rare-earth doped $CaNb_2O_6$, the rare-earth ions partially substitutes for Ca^{2+} in the host crystal lattices, which causes charge imbalance in the sublattice. The structure consists of calcium and niobium atoms surrounded by oxygen atoms in a polyhedral arrangement. The polyhedral shares corners and edges to form a chainlike network throughtout the solid[16]. The undoped $CaZnNb_2O_6$ are reported to produce blue luminescence under NUV excitation, hence this can be useful for the NUV based pc-white LEDs.

1.7 Aim of this study

1. To synthesize Eu^{3+} and Zn^{2+} co-doped $CaNb_2O_6$ phosphors using solid state reaction technique.
2. To carry out TGA analysis to know the sintering temperature.
3. Determining the crystal structure and crystallite size by using X-Ray Diffraction
5. To study the excitation initially and then measured photoluminescence (PL) properties of $CaZnNb_2O_6:Eu^{3+}$ based on excitation results.
6. To calculate chromaticity coordinates.
7. To know the potential utility of the phosphor in solid state lighting applications

References

1. Y. Chen, M. Gong, G. Wang, Q. Su, Appl. Phys. Lett. 91 (2007) 071117.
2. T.R.N. Kutty, A. Nag, J. Mater. Chem. 13 (2003) 2271.
3. T. Nishida, T. Ban, N. Kobayashi, Appl. Phys. Lett. 82 (2003) 3817.
4. S. Neeraj, Chem. Phys. Lett. 387 (2004) 2.
5. Nag A, Kutty T R N.. Journal of Materials Chemistry, 2004, 14(10): 1598.
6. Taylor and francis group,2006, Phosphor handbook,Shigeo Shiyonoya, chapter one , Introduction to rare-earths.
7. Soumonni Ogundiran, Thesis, Georgia Institute of Technology, April 2004, pg5,6, 44,45,46,54.
8. http://scienceworld.wolfram.com/physics/Fluorescence.html
9. Karl A. Franz, Wolfgang G. Kehr, Alfred Siggel, Jürgen Wieczoreck, and Waldemar Adam "Luminescent Materials" in Ullmann's Encyclopedia of Industrial Chemistry 2002, Wiley-VCH, Weinheim.
10. Luminescence from theory to applications, Cess.R.Ronda, Wiley and sons,2008, chapter 1.
11. http://www.tf.uni-kiel.de/matwis/amat/admat_en/kap_5/advanced/t5_2_4.html
12. http://www.stanfordmaterials.com/Long-Phor-App.html
13. http://en.wikipedia.org/wiki/Field_emission_display
14. http://www.toshiba-tmat.co.jp/eng/product/ligh.htm
15. Di et al. / Journal of Alloys and Compounds 536 (2012) 20.
16. The Americal mineralologist, Vol.55, 1970.

.

CHAPTER 2

Characterization techniques and sample preparation

The phosphors prepared by the different techniques were characterized by scanning electron microscopy, x-ray diffraction and photoluminescence spectra. The theory of these techniques with the experimental layout is discussed in this chapter.

2.1 X-Ray diffraction

X-ray crystallography is a method of determining the arrangement of atoms within a crystal, in which a beam of X-rays strikes a crystal and causes the beam of light to spread into many specific directions. From the angles and intensities of these diffracted beams, a crystallographer can produce a three-dimensional picture of the density of electrons within the crystal. From this electron density, the mean positions of the atoms in the crystal can be determined, as well as their chemical bonds, their disorder and various other information.

Figure 2.1: XRD instrument

Since many materials can form crystals—such as salts, metals, minerals, semiconductors, as well as various inorganic, organic and biological molecules—X-ray crystallography has been fundamental in the development of many scientific fields. In its first decades of use, this method determined the size of atoms, the lengths and types of chemical bonds, and the atomic-scale differences among various materials, especially minerals and alloys. The method also revealed the structure and function of many biological molecules, including vitamins, drugs, proteins and nucleic acids such as DNA. X-ray crystallography is still the chief method for characterizing the atomic structure of new materials and in discerning materials that appear similar by other experiments. X-ray crystal structures can also account for unusual electronic or elastic properties of a material, shed light on chemical interactions and processes, or serve as the basis for designing pharmaceuticals against diseases.

In an X-ray diffraction measurement, a crystal is mounted on a goniometer and gradually rotated while being bombarded with X-rays, producing a diffraction pattern of regularly spaced spots known as *reflections*. The two-dimensional images taken at different rotations are converted into a three-dimensional model of the density of electrons within the crystal using the mathematical method of Fourier transforms, combined with chemical data known for the sample. Poor resolution (fuzziness) or even errors may result if the crystals are too small, or not uniform enough in their internal makeup.

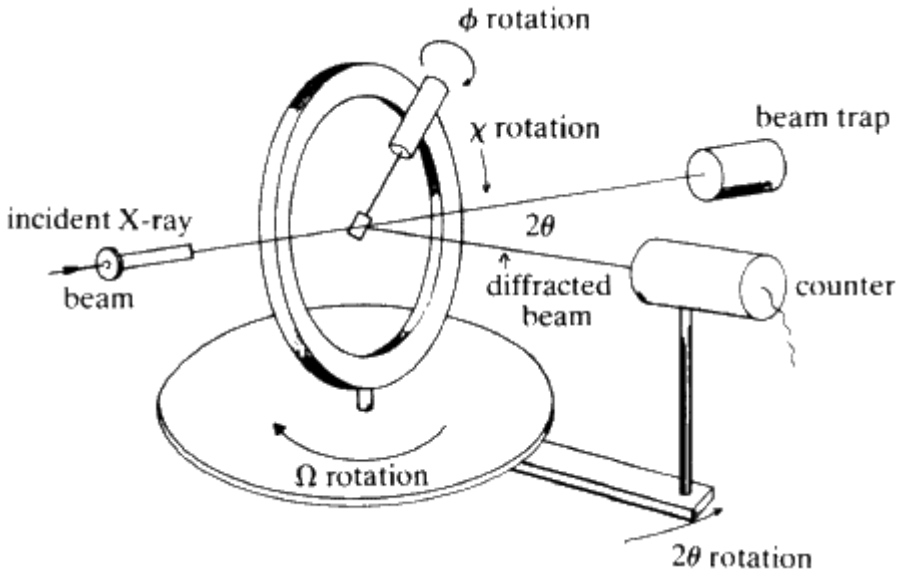

Figure 2.2: Goniometer [1]

X-ray crystallography is related to several other methods for determining atomic structures. Similar diffraction patterns can be produced by scattering electrons or neutrons, which are likewise interpreted as a Fourier transform. If single crystals of sufficient size cannot be obtained, various other X-ray methods can be applied to obtain less detailed information; such methods include fiber diffraction, powder diffraction and small-angle X-ray scattering (SAXS). If the material under investigation is only available in the form of nanocrystalline powders or suffers from poor crystallinity, the methods of electron crystallography can be applied for determining the atomic structure.

Crystals are regular arrays of atoms, and X-rays can be considered waves of electromagnetic radiation. Atoms scatter X-ray waves, primarily through the atoms' electrons. Just as an ocean wave striking a lighthouse produces secondary circular waves emanating from the lighthouse, so an X-ray striking an electron produces secondary spherical waves

emanating from the electron. This phenomenon is known as elastic scattering, and the electron (or lighthouse) is known as the *scatterer*. A regular array of scatterers produces a regular array of spherical waves. Although these waves cancel one another out in most directions through destructive interference, they add constructively in a few specific directions, determined by Bragg's law:

$$2d \sin\theta = n\lambda$$

Here *d* is the spacing between diffracting planes, $\theta$is the incident angle, *n* is any integer, and λ is the wavelength of the beam. These specific directions appear as spots on the diffraction pattern called *reflections*. Thus, X-ray diffraction results from an electromagnetic wave (the X-ray) impinging on a regular array of scatterers (the repeating arrangement of atoms within the crystal).**[2]**

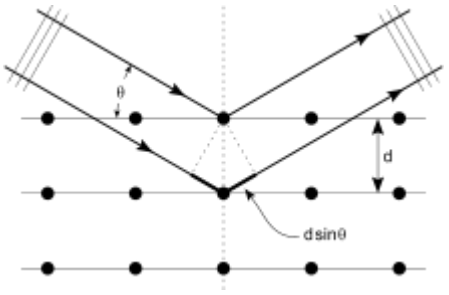

Figure 2.3: Bragg's diffraction

The incoming beam (coming from upper left) causes each scatterer to re-radiate a small portion of its intensity as a spherical wave. If scatterers are arranged symmetrically with a separation *d*, these spherical waves will be in sync (add constructively) only in directions where their path-length difference 2*d* sin θ equals an integer multiple of the wavelength λ. In that case, part of the incoming beam is deflected by an angle 2θ, producing a *reflection* spot in the diffraction pattern.**[3]**

2.2 Scanning Electron microscope

A **scanning electron microscope** (**SEM**) is a type of electron microscope that images a sample by scanning it with a beam of electrons in a raster scan pattern. The electrons interact with the atoms that make up the sample producing signals that contain information about the

sample's surface topography, composition, and other properties such as electrical conductivity.

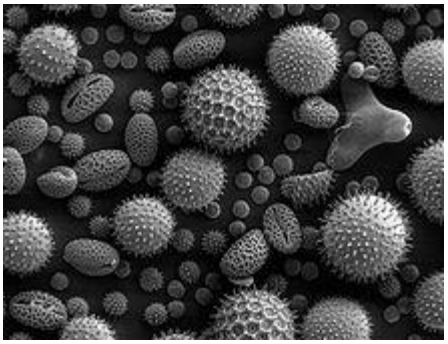

Figure 2.3: SEM image of pollen grains

These pollen grains taken on an SEM show the characteristic depth of field of SEM micrographs.

2.2.1 Principles and capacities

The types of signals produced by a SEM include secondary electrons, back-scattered electrons (BSE), characteristic X-rays, light (cathodoluminescence), specimen current and transmitted electrons. Secondary electron detectors are common in all SEMs, but it is rare that a single machine would have detectors for all possible signals. The signals result from interactions of the electron beam with atoms at or near the surface of the sample. In the most common or standard detection mode, secondary electron imaging or SEI, the SEM can produce very high-resolution images of a sample surface, revealing details less than 1 nm in size. Due to the very narrow electron beam, SEM micrographs have a large depth of field yielding a characteristic three-dimensional appearance useful for understanding the surface structure of a sample. This is exemplified by the micrograph of pollen shown above. A wide range of magnifications is possible, from about 10 times (about equivalent to that of a powerful hand-lens) to more than 500,000 times, about 250 times the magnification limit of the best light microscopes. Back-scattered electrons (BSE) are beam electrons that are reflected from the sample by elastic scattering. BSE are often used in analytical SEM along with the spectra made from the characteristic X-rays. Because the intensity of the BSE signal is strongly related to the atomic number (Z) of the specimen, BSE images can provide information about the distribution of different elements in the sample. For the same reason, BSE imaging can image colloidal gold immuno-labels of 5 or 10 nm diameter, which would

otherwise be difficult or impossible to detect in secondary electron images in biological specimens. Characteristic X-rays are emitted when the electron beam removes an inner shell electron from the sample, causing a higher-energy electron to fill the shell and release energy. These characteristic X-rays are used to identify the composition and measure the abundance of elements in the sample.

2.2.2 Scanning process and image formation

In a typical SEM, an electron beam is thermionically emitted from an electron gun fitted with a tungsten filament cathode. Tungsten is normally used in thermionic electron guns because it has the highest melting point and lowest vapour pressure of all metals, thereby allowing it to be heated for electron emission, and because of its low cost. Other types of electron emitters include lanthanum hexaboride (LaB_6) cathodes, which can be used in a standard tungsten filament SEM if the vacuum system is upgraded and field emission guns (FEG), which may be of the cold-cathode type using tungsten single crystal emitters or the thermally assisted Schottky type, using emitters of zirconium oxide.

The electron beam, which typically has an energy ranging from 0.2 keV to 40 keV, is focused by one or two condenser lenses to a spot about 0.4 nm to 5 nm in diameter. The beam passes through pairs of scanning coils or pairs of deflector plates in the electron column, typically in the final lens, which deflect the beam in the *x* and *y* axes so that it scans in a raster fashion over a rectangular area of the sample surface.

When the primary electron beam interacts with the sample, the electrons lose energy by repeated random scattering and absorption within a teardrop-shaped volume of the specimen known as the interaction volume, which extends from less than 100 nm to around 5 µm into the surface. The size of the interaction volume depends on the electron's landing energy, the atomic number of the specimen and the specimen's density. The energy exchange between the electron beam and the sample results in the reflection of high-energy electrons by elastic scattering, emission of secondary electrons by inelastic scattering and the emission of electromagnetic radiation, each of which can be detected by specialized detectors. The beam current absorbed by the specimen can also be detected and used to create images of the distribution of specimen current. Electronic amplifiers of various types are used to amplify the signals, which are displayed as variations in brightness on a computer monitor (or, for vintage

models, on a cathode ray tube). Each pixel of computer videomemory is synchronised with the position of the beam on the specimen in the microscope, and the resulting image is therefore a distribution map of the intensity of the signal being emitted from the scanned area of the specimen. In older microscopes image may be captured by photography from a high-resolution cathode ray tube, but in modern machines image is saved to a computer data storage [10].

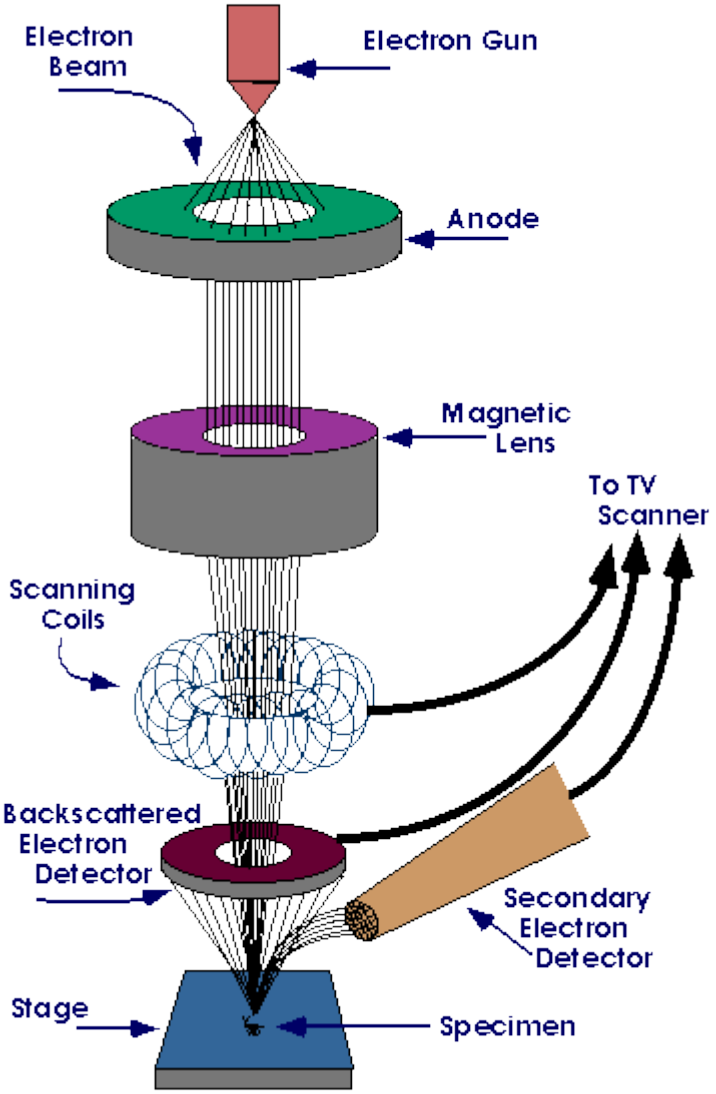

Figure 2.4: SEM Working

2.3 Photoluminescence

Photoluminescence spectroscopy is a contact-less, versatile, non-destructive method

of probing the electronic structure of a material. A Laser beam impinges on a sample, where it is absorbed. The excess energy brought to the material can be dissipated through the emission of light, or luminescence. Photoluminescence (PL) is thus the spontaneous emission of light from a material under optical excitation. This light can be collected and analyzed spectrally, spatially and also temporally. In fact, PL spectroscopy gives information only on the low- lying energy levels of the investigated system. In semiconductor systems, the most common radiative transition is between states in the conduction and valence bands, with the energy difference being known as the bandgap. During a PL spectroscopy experiment, excitation is provided by laser/Xe light with an energy much larger than the optical bandgap. The photo- excited carriers consist of electrons and holes, which relax toward their respective band edges and recombine by emitting light at the energy of the bandgap. But, radiative transitions in semiconductors may also involve localized defects or impurity levels. In that case, the analysis of the PL spectrum leads to the identification of specific defects or impurities, and the magnitude of the PL signal allows determining their concentration. Finally, higher-energy optical transitions can be studied by means of photoluminescence excitation spectroscopy (PLE). In this latter configuration the detection is fixed on the emission line of the semiconductor system while the excitation light energy is varied. When it matches the energy of an optical transition in the absorption spectrum of the semiconductor, the PL signal increases. PLE is thus analogous to absorption spectroscopy and identical to it in the specific case where nonradiative relaxation processes are negligible. The recombination of the photo- excited carriers can involve both radiative and nonradiative processes. The respective rates of radiative and nonradiative recombination can be estimated from a careful analysis of the temperature variation of the PL intensity and PL decay time [6]. In semiconductor systems like quantum wells or quantum dots, the photoluminescence quantum yield is approximately constant up to temperatures of about 50-70K. At higher temperatures nonradiative recombination channels are activated and the PL intensity decreases exponentially. Apart the advantageous simplification of the underlying physics, low temperatures appear unavoidable for the optical study of semiconductor-based nanostructures [7].

In the present study following instruments were used for the optical characterization of the samples Edinburgh Instruments combined steady state luminescence Spectrometer.

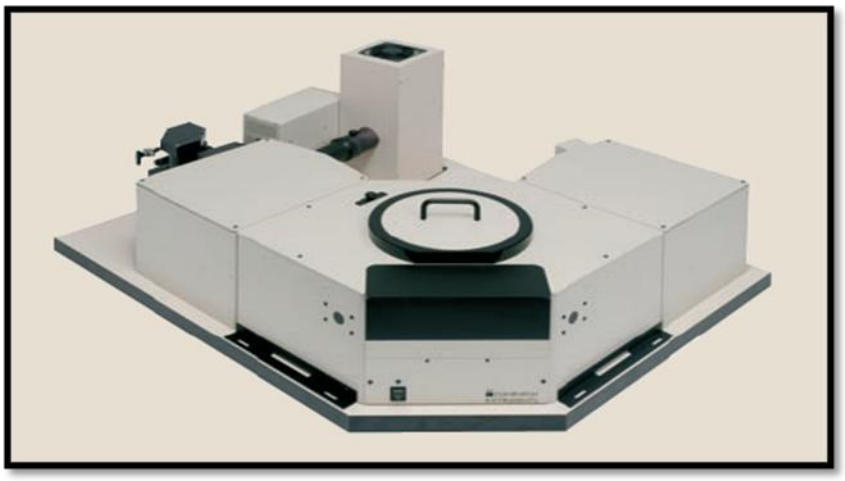

Figure 2.5: Edinberg Specrometer

The simple ray diagram of functioning of instrument is given in the figure 2.5 . First of all excitation source, xenon flash lamp, is switched on. Energy from the source is focused by the spherical mirror onto the excitation monochromator. The majority of excitation beam is transmitted to the phosphor sample. The sample gets excited and energy emitted from it is once again focused by spherical mirror onto the emission monochromator. The angles of the gratings used in the excitation and emission monochromators are controlled by stepper motors. The emitted light is detected by a sensitive Photomultiplier tube (PMT) with high signal to noise ratio. The operation is software controlled. The excitation and emission wavelength (or range of excitation wavelengths in case of PL Excitation spectra or emission

wavelength in case of PL emission spectra), the excitation and emission slit width and wavelength scan speed can all be controlled through software. The resultant PL spectra are shown in a computer screen which can be saved and printed.

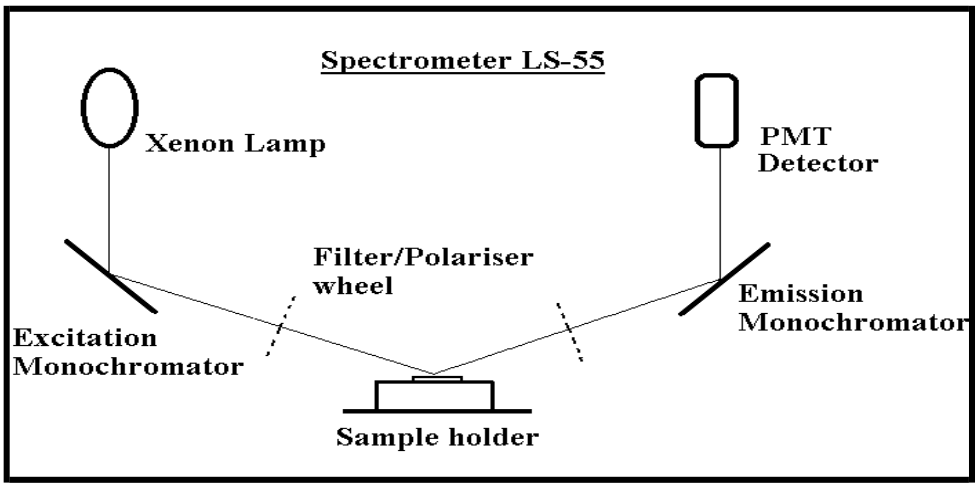

Figure 2.6: Functional Diagram of LS-55 Luminescence Spectrometer

The excitation and emission monochromators can be scanned over their ranges independently, synchronously or driven to selected points in their ranges. The spectral ranges of the monochromators are:

- Excitation monochromator 200 nm to 800 nm
- Emission monochromator 200 nm to 900 nm

2.4 Thermogravimetric analysis

Thermogravimetric analysis or **thermal gravimetric analysis** is a type of testing performed on samples that determines changes in weight in relation to a temperature program in a controlled atmosphere. Such analysis relies on a high degree of precision in three measurements: weight, temperature, and temperature change. As many weight loss curves look similar, the weight loss curve may require transformation before results may be interpreted. A derivative

weight loss curve can identify the point where weight loss is most apparent. Again, interpretation is limited without further modifications and deconvolution of the overlapping peaks may be required. To determine composition and purity one must take the mass of the substance in the mixture by using thermal gravimetric analysis. Thermal gravimetric analysis is the act of heating a mixture to a high enough temperature so that one of the components decomposes into a gas, which dissociates into the air. It is a process that utilizes heat and stoichiometry ratios to determine the percent by mass ratio of a solute. If the compounds in the mixture that remain are known, then the percentage by mass can be determined by taking the weight of what is left in the mixture and dividing it by the initial mass. Knowing the mass of the original mixture and the total mass of impurities liberating upon heating, the stoichiometric ratio can be used to calculate the percent mass of the substance in a sample. TGA is commonly employed in research and testing to determine characteristics of materials such as polymers, to determine degradation temperatures, absorbed moisture content of materials, the level of inorganic and organic components in materials, decomposition points of explosives, and solvent residues. It is also often used to estimate the corrosion kinetics in high temperature oxidation.

Simultaneous TGA-DTA/DSC measures both heat flow and weight changes (TGA) in a material as a function of temperature or time in a controlled atmosphere. Simultaneous measurement of these two material properties not only improves productivity but also simplifies interpretation of the results. The complementary information obtained allows differentiation between endothermic and exothermic events with no associated weight loss (e.g. melting and crystallization) and those that involve a weight loss (e.g. degradation).

2.4.1 Equipment

The analyzer usually consists of a high-precision balance with a pan (generally platinum) loaded with the sample. That pan resides in a furnace and is heated or cooled during the experiment. A different process using a quartz crystal microbalance has been devised for measuring smaller samples on the order of a microgram (versus milligram with conventional TGA) [8]. The sample is placed in a small electrically heated oven with a thermocouple to accurately measure the temperature. The atmosphere may be purged with an inert gas to prevent oxidation or other undesired reactions. A computer is used to control the instrument.

2.4.2 Methodology

TGA is a process that utilizes heat and stoichiometry ratios to determine the percent by mass of a solute. Analysis is carried out by raising the temperature of the sample gradually and plotting weight (percentage) against temperature. The temperature in many testing methods routinely reaches 1000°C or greater. After the data are obtained, curve smoothing and other operations may be done to find the exact points of inflection.

A method known as hi-resolution TGA is often employed to obtain greater accuracy in areas where the derivative curve peaks. In this method, temperature increase slows as weight loss increases. This is to more accurately identify the exact temperature where a peak occurs. Several modern TGA devices can vent burn off to an infrared spectrophotometer to analyze composition [9].

Figure 2.7: TGA equipment

2.5 Sample preparation

The Eu^{3+} and Zn^{2+} doped $CaNb_2O_6$ powders were prepared by using solid state reaction method. The starting materials niobium pentoxide (Nb_2O_5), zinc oxide (ZnO), calcium carbonate ($CaCO_3$) and europium oxide (Eu_2O_3) (A.R grade) were weighed in the stoichiometric ratio and ground in an agate mortar for an hour. TGA-DSC analysis was used to determine the suitable heat treatment. Based on the TGA-DSC results, the sample was placed in an alumina crucible and sintered in an electric furnace at 1050 ^oC for 6 hours. The flow charts of the heat treatment and sample preparation are depicted in figure 2.8 and 2.9, respectively.

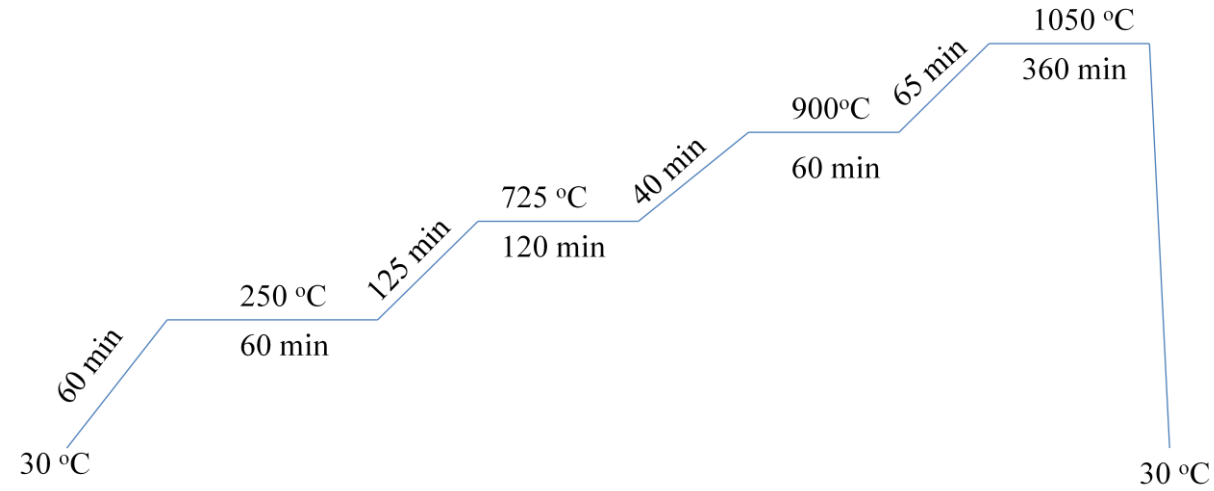

.

Figure 2.8: Reaction conditions of $Ca_{0.9-x}Zn_{0.1}Nb_2O_6$:Eu

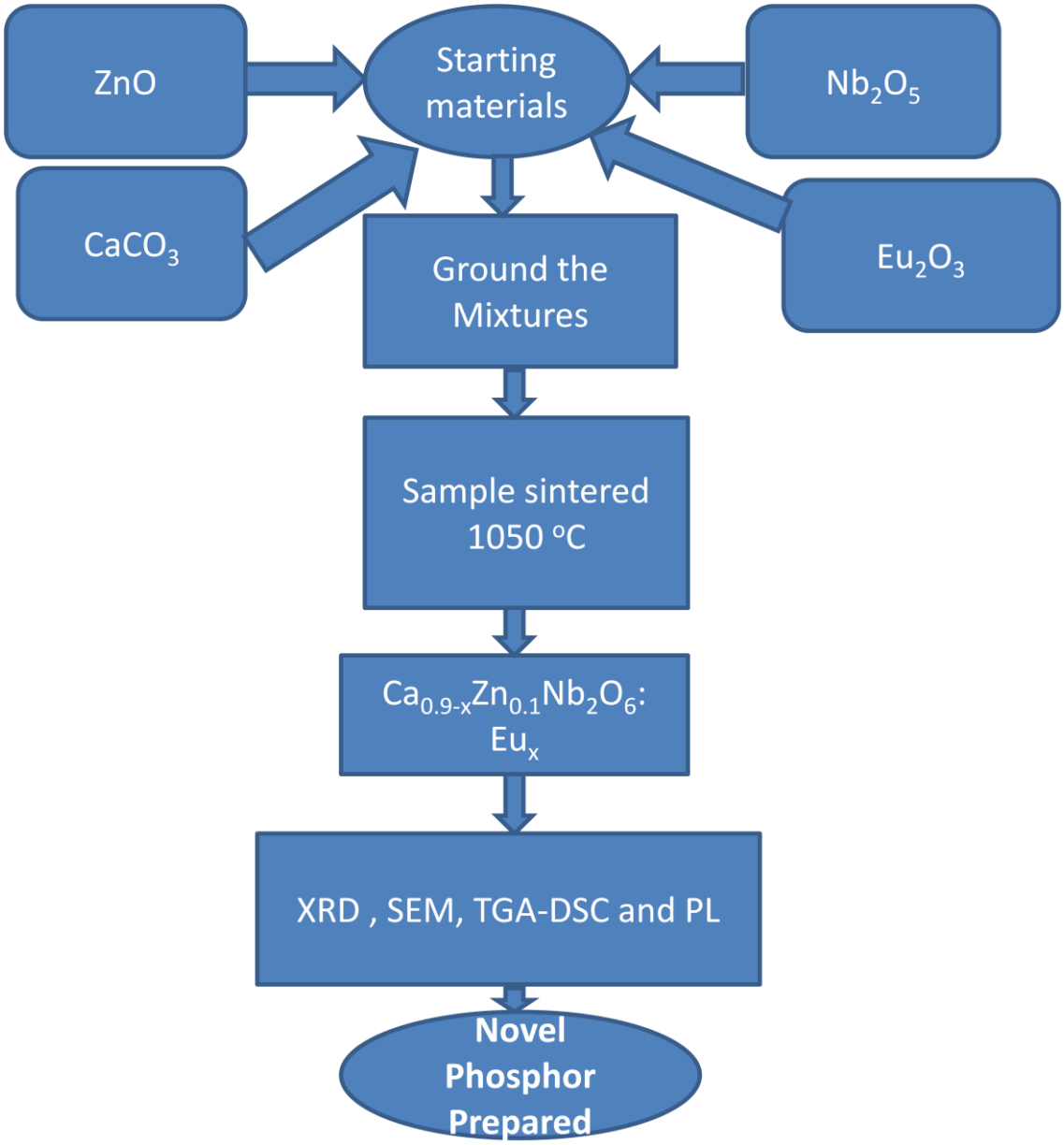

Figure 2.9 Sample Preparation of $Ca_{0.9-x}Zn_{0.1}Nb_2O_6$: Eu_x

References

1. https://www.google.co.in/search?hl=en&cp=8&gs_id=84q&xhr=t&q=x-ray+diffraction&bav=on.2,or.r_gc.r_pw.r_cp.r_qf.,cf.osb&biw=1366&bih=643&um=1&ie=UTF-8&tbm=isch&source=og&sa=N&tab=wi&ei=CS_CT7rQPMjQrQev3bTnCQ
2. http://en.wikipedia.org/wiki/X-ray_crystallography
3. http://en.wikipedia.org/wiki/X-ray_crystallography
4. S. Shi, J. Gao, J. Zhou, Opt. Mater. 30 (2008) 1616.
5. Z. Wang, H. Liang, J. Wang, M. Gong, Q. Su, Appl. Phys. Lett. 89 (2006) 071921.
6. http://serc.carleton.edu/research_education/geochemsheets/techniques/SEM.html
7. http://nobelprize.org/educational/physics/microscopes/tem/index.html
8. Mansfield, E.; Kar, A.; Quinn, T. P.; Hooker, S. A. (2010) *Analytical Chemistry* 82 (24): 101116152615035
9. http://en.wikipedia.org/wiki/Thermogravimetric_analysis
10. http://en.wikipedia.org/wiki/Scanning_electron_microscope

CHAPTER 3

Results and discussions

3.1 TGA-DSC analysis

On the basis of TGA-DSC results as shown in figure 3.1 the sample showed two broad endothermic peaks, the first one at 725 ^{o}C and the second at around 810 ^{o}C due to the mass loss. Considering the results of the TGA-DSC, the sample was sintered at 1050 ^{o}C as it is getting stable near 1050 ^{o}C.

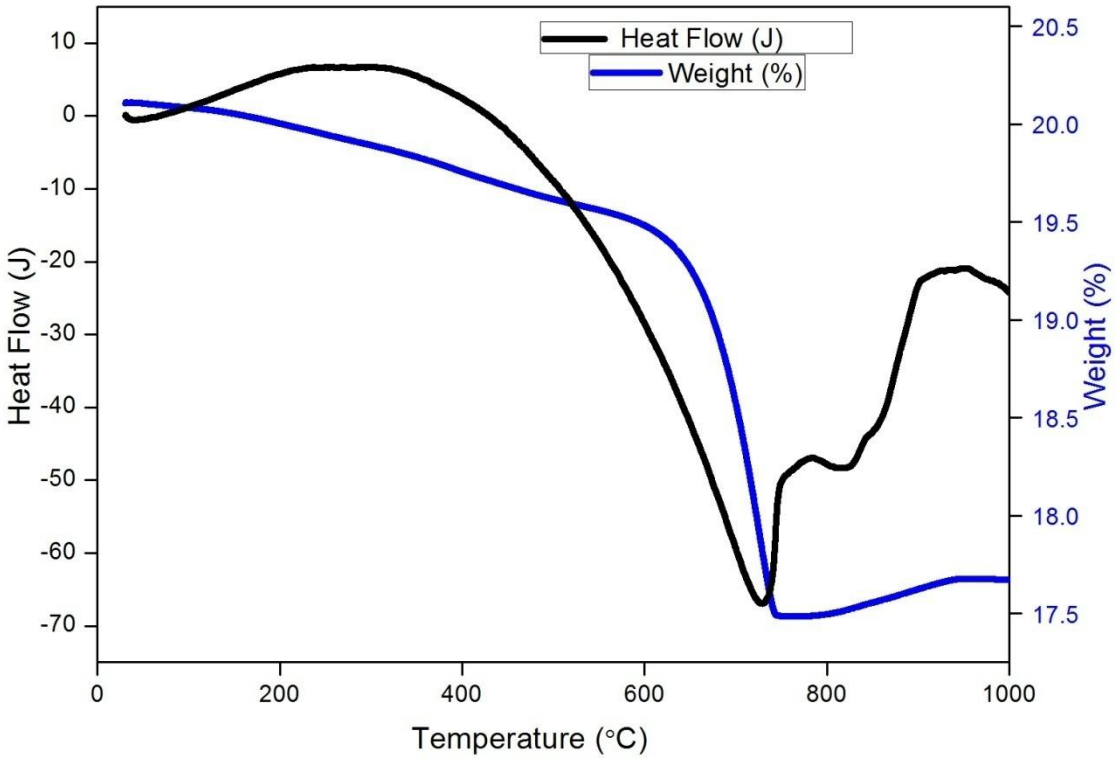

Figure 3.1: TGA/DSC of unsintered $Ca_{0.9-x}Zn_{0.1}Nb_2O_6$: Eu_x

3.2 XRD

The synthesized $Ca_{0.9-x}Zn_{0.1}Nb_2O_6$: Eu_x samples were characterized by powder X-ray diffraction. The measurements were carried with CuKα radiation(1.5406 Å). The XRD patterns as shown in figure 3.2 were analyzed and found to be in good agreement by comparing with the reported ones. The average crystallite size calculated by using Scherrer's relation: $d=0.9\lambda/\beta\cos\theta$, wherein λ is the wavelength of X-rays and β is the corrected full width at half maxima and the crystallite size obtained is ~57 nm.

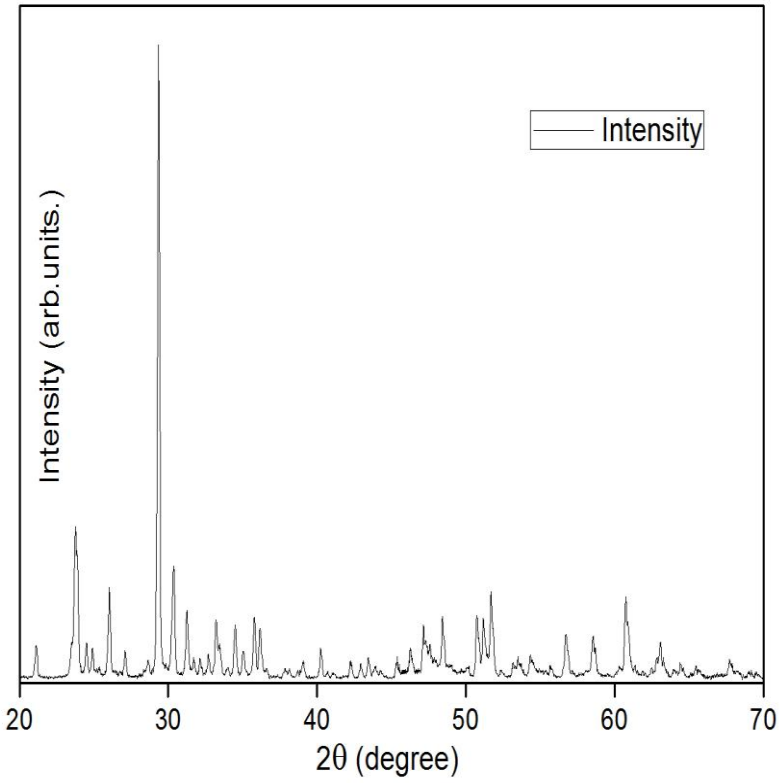

Fig. 3.2: XRD pattern of $Ca_{0.9-x}Zn_{0.1}Nb_2O_6$: Eu_x

3.3 SEM

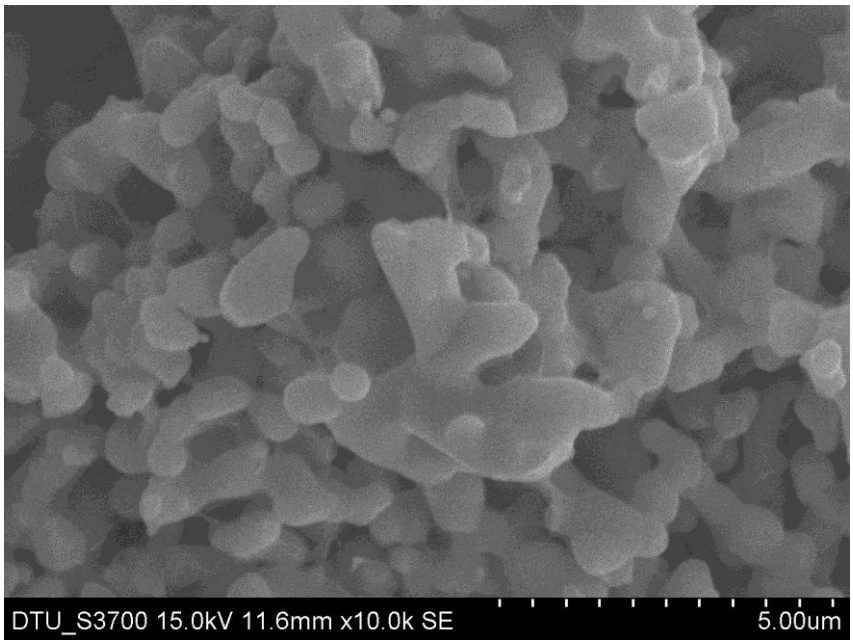

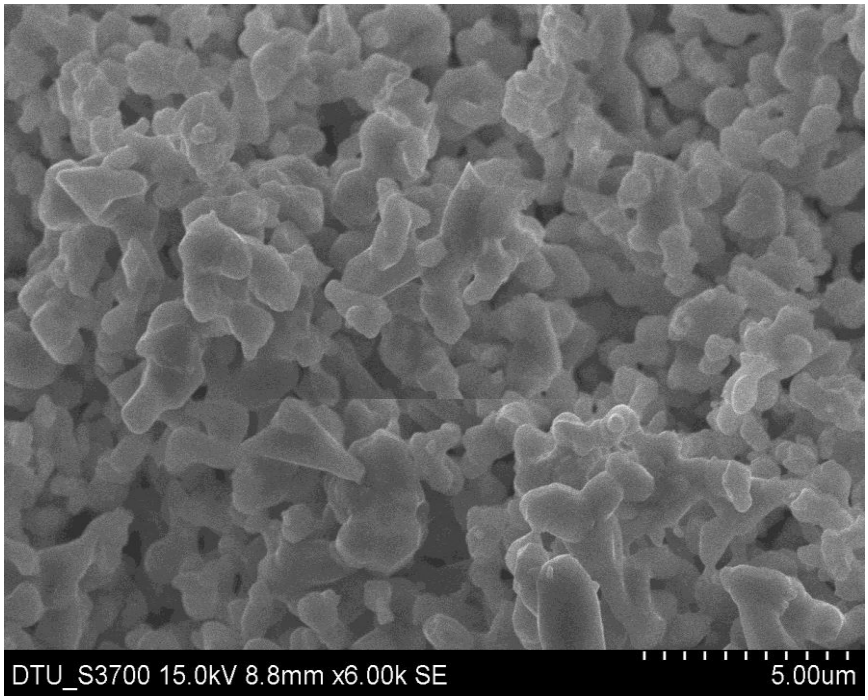

Figure 3.3: Scanning electron images of $Ca_{0.9-x}Zn_{0.1}Nb_2O_6$: Eu_x phosphors

Scanning electron microscopy has been used to study the morphology and particle size of the phosphor powder for the $Ca_{0.9-x}Zn_{0.1}Nb_2O_6$: Eu_x samples. The particles show polyhedral shape morphology with agglomerated nature as shown in the figure 3.3**.** The particle size for the phosphor powder shows an extension from sub-micrometers to micrometers.

3.4 Excitation spectra

The excitation spectra exhibit one broad band at 266 nm and a sharp peak at 395 nm as shown in figure 3.4. It is favorable to the red emission of Eu^{3+}.Under 240–300 nm excitation, the Eu^{3+} ions are bump to CTB state, and then decay to the 4f level of Eu^{3+} ions. This broadband is related to the O^{2-}-Eu^{3+} charge transfer band (CTB), which is caused by the electron transfer from 2p orbits of O^{2-} ions to 4f shells of Eu^{3+}ions.The excitation bands from near UV to visible are strong, the excitation peak at about 394 nm in particular, which is due to the transitions of Eu^{3+} is related to the intraconfigurational 4f-4f transitions of Eu^{3+} ions into host lattices, which can be assigned to $^7F_0$-$^5L_6$ as shown in figure 3.4. Other narrow excitation peaks are 4f→4f transition absorption of Eu^{3+}. The 4f orbital is shielded from the surroundings by the filled $^5s_2$ and $^5p_2$ orbitals [3-5]. Therefore the influence of the host lattice on the optical transitions within the $4f^n$ configuration is small and 4f-4f transitions are sharp lines [2].

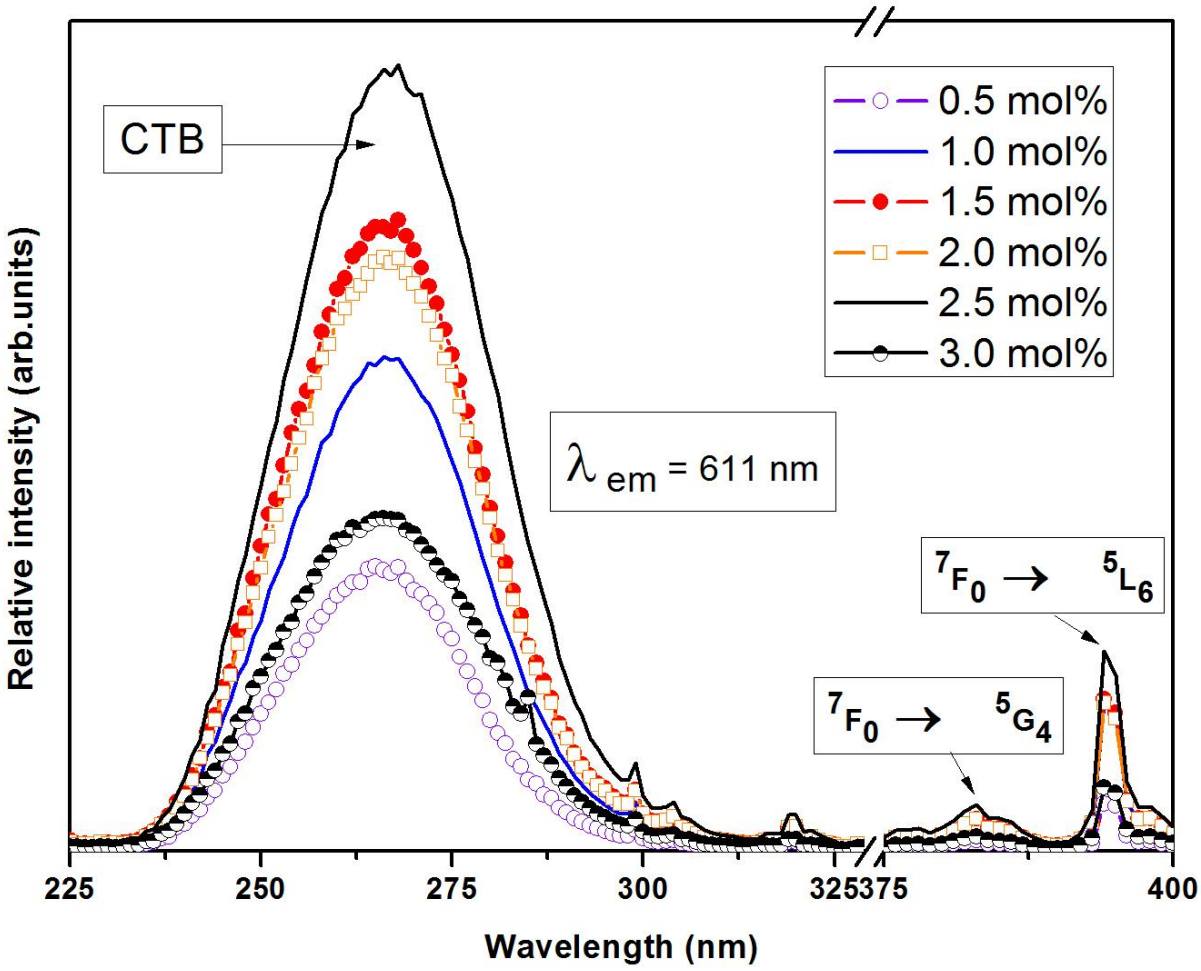

Figure 3.4: Excitation spectra of $Ca_{0.9-x}Zn_{0.1}Nb_2O_6$: Eu_x phosphors

3.5 Emission Spectra

Due to the availability of TGA-DSC results only till 1050 ^oC, the sample was sintered at 1050, 1200 and 1300 ^oC to check the emission intensity of all the three samples at the 1 mole% and as shown in figure 3.5 Among the three different sintering temperatures, it was found that 1050 ^oC exhibited the highest emission peak. Therefore, based on the comparative results, remaining samples were also sintered at 1050 ^oC to record the emission spectra.

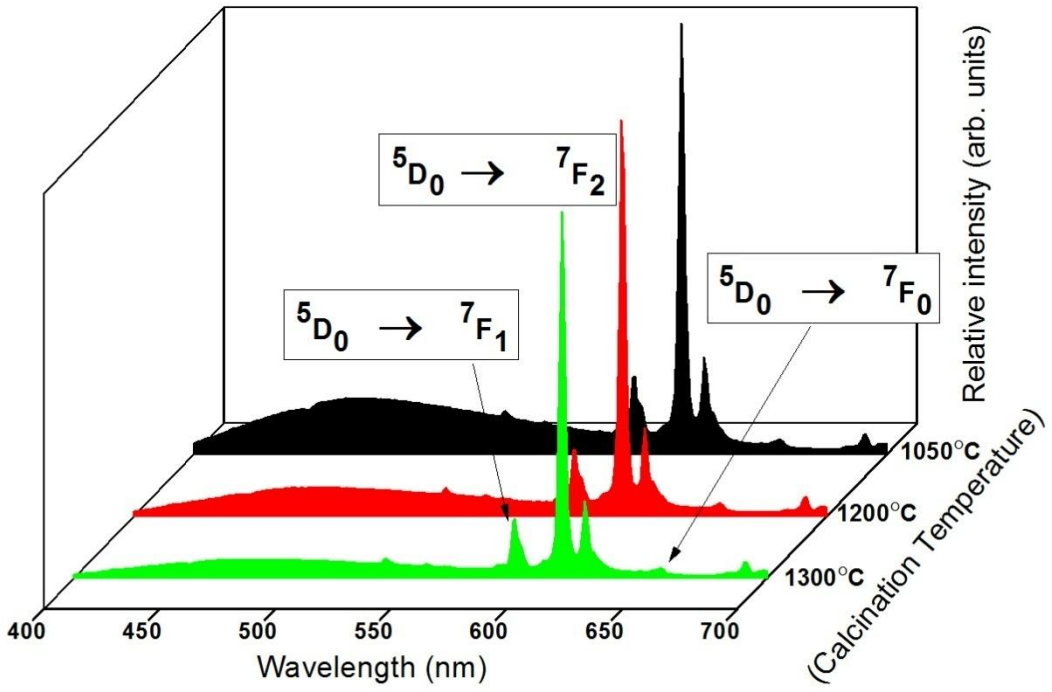

Figure 3.5: Emission spectra of $Ca_{0.9-x}Zn_{0.1}Nb_2O_6$: Eu_x at different calcinations temperatures

There are two major excitation peaks, one is 268nm and another one is at 395 nm as revealed by the excitation spectra of all the mole percentages.

3.5.1 Emission Spectra at 266 nm

The emission lines can be attributed to the optical transitions from the excited state $^5D_0$ –^{7} F_J levels (J=0, 1, 2, 3, or 4) of the $4f^6$ configuration of Eu^{3+} ions. According to the Judd-Ofelt theory, transitions to even J-numbers have a much higher intensity than those to corresponding neighboring uneven J-numbers [6]. In addition, the $^5D_0$ –^{7} F_J emissions is very suitable to survey the transition probabilities of the sharp spectral features of the rare earths. Generally, if a rare-earth ion occupies a site with inversion symmetry in the crystal lattice, optical transitions between levels of the $4f^n$ configuration are strictly forbidden as electric-dipole transition. They can only occur as (the much weaker) magnetic-dipole transitions which obey the selection rule J=0, ±1 (but J=0 to J=0 forbidden) or as vibronic electric-dipole transitions. If there is no inversion symmetry at the site of the rare-earth ion, the uneven crystal field component can mix opposite-parity states into the $4f^n$-configurational levels. The electric-dipole transitions are now no longer strictly forbidden and appear as (weak) lines in the spectrum, the so-called forced electric-dipole transitions. Some transitions

(those with J=0, ±2) are hypersensitive to this effect. Even for small deviations from inversion symmetry, they appear dominant in the spectrum [8]. A strong red emission band centered at 611 nm can be observed in figure 3.6 for $Ca_{0.9-x}Zn_{0.1}Nb_2O_6$: Eu_x samples. The peaks of excitation was associated with charge transfer bands of $[NbO_6]^7$ in the $CaZnNb_2O_6:Eu^{3+}$ system at about 266 nm. Here, the edge-shared NbO_6 groups are efficient luminescent centers for the blue emission [9]. The Eu^{3+} :$[NbO_6]^7$ group exhibited the red emission about 613 nm excited at ex = 266 nm that is the emissions are due to the energy transfer from the niobate groups to Eu^{3+} ions as shown in figure 4.8 . This luminescence effect depends on the Nb–O–Nb bonding that the conduction band is composed of Nb^{5+} 4d orbitals, and the valence band of O^{2-} 2p orbitals between the corner-sharing octahedral which is also responsible for broader region emission below 590 nm [10]. This broader region region emission due to charge transfer (as explained above) to niobate groups could be supported from the undoped $CaZnNb_2O_6$ sample exhibiting blue emission as shown in the figure 3.6.

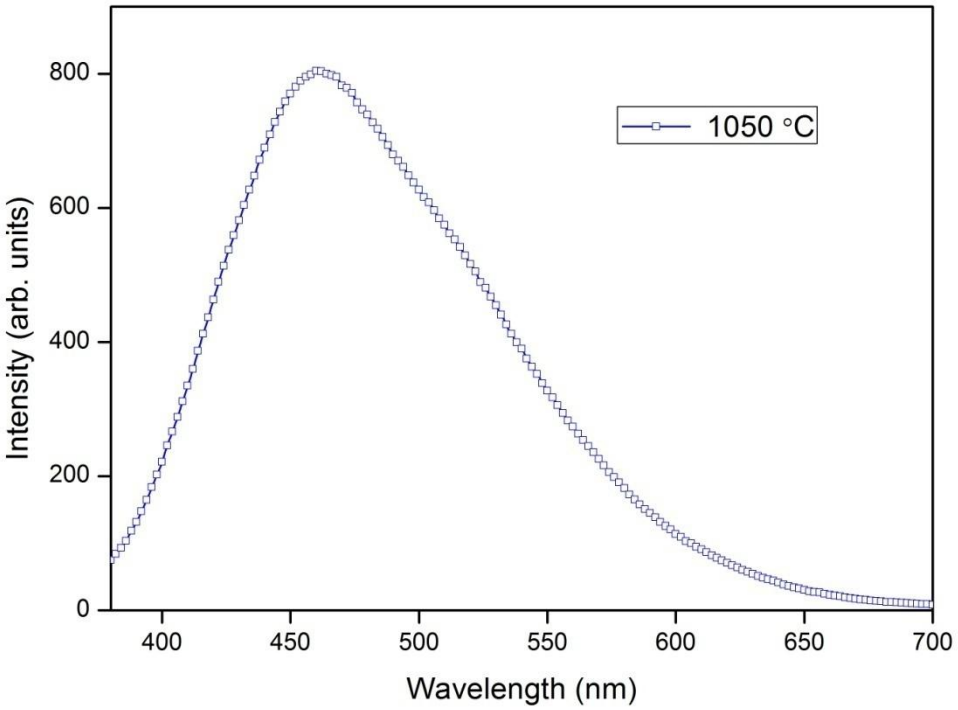

Figure 3.6: Undoped $Ca_{0.9-x}Zn_{0.1}Nb_2O_6$: Eu_x emission spectrum

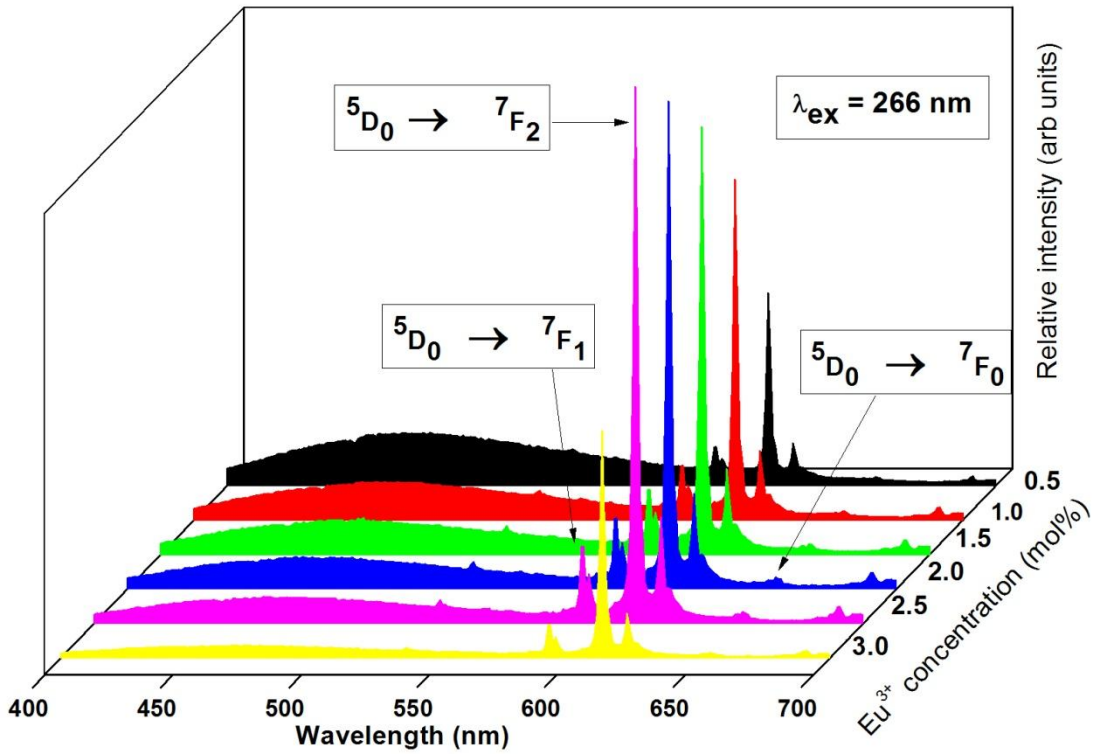

Figure 3.7: Emission spectra of $Ca_{0.9-x}Zn_{0.1}Nb_2O_6$: Eu_x phosphors at 266 nm excitation

Therefore, as the Eu^{3+} concentration increases, $[NbO_6]^7$ emission decreases monotonically whereas Eu^{3+} emission first increases gradually due to more energy transfer from $[NbO_6]^7$ groups to Eu^{3+} reaching to a maximum at 2.5mol% as shown in the figure 3.8 and then decreases due to concentration quenching that occurs in this case when Eu^{3+} concentrations are above 2.5 mol%, which is caused by the effect of energy exchange between the Eu^{3+} ions as the distance between them decreases with the increasing Eu^{3+} ion concentrations, enhancing the energy depletion rate and causing the decay time to decrease.

The emission spectra was dominated by the two transitions of $^5D_0 -^7 F_1$ (595 nm) and $^5D_0 -^7 F_2$ (611 nm) as shown in figure 3.7[11]. It is well known that $^5D_0 -^7 F_1$ is a magnetic dipole transition in nature and is also independent of the crystallographic site of the Eu^{3+} ions. $^5D_0 -^7 F_2$ is an electric dipole transition implying Eu^{3+} ions occupy the noncentrosymmetric sites. Therefore, doping the Eu3+ ions made the ions distributing throughout the noncentrosymmetric sites in the host of $Ca_{0.9-x}Zn_{0.1}Nb_2O_6$: Eu_x, the $^5D_0 -^7 F_2$ (610–620 nm) transition dominates, but other lines are also present. $^5D_0 -^7 F_1$ (590–600 nm), that can be attributed to the magnetic-dipole emission, but overruled by the hypersensitive forced electric-dipole emission $^5D_0 -^7 F_2$ (610–620 nm), which indeed is dominant in our case [7].

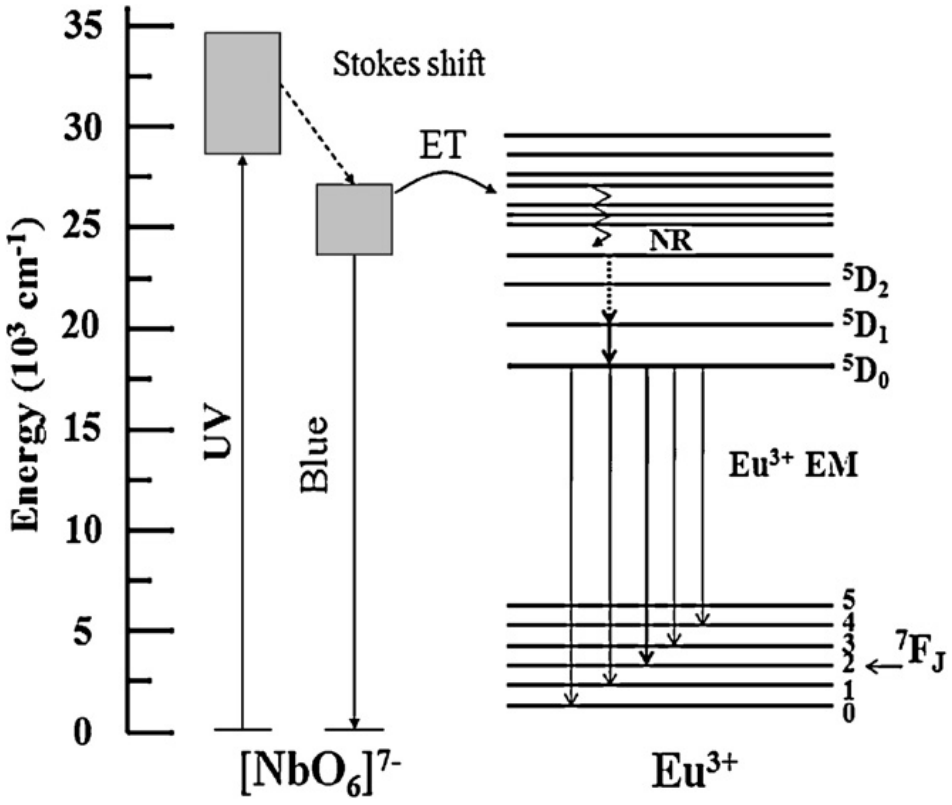

Fig.3.8: Emission and energy transfer process at 266 nm in $Ca_{0.9-x}Zn_{0.1}Nb_2O_6$: Eu_x

3.5.2 Emission spectra at 395 nm

From the excitation spectra, among all the 4f-4f transitions, the strong emission line is at 394 nm attributed to $^7F_0$-$^5L_6$ transition in the NUV region**.** Figure 3.9 shows the emission spectrum of the $Ca_{0.9-x}Zn_{0.1}Nb_2O_6$: Eu_x that was excited by 394 nm and exhibited a well known characteristic Eu^{3+} emission. It consists of several emission lines as shown in figure 3.9, originating from the transitions of excited states $^5D_0$ to ground state ^7F_j (j=0,1,2,3) in the $4f^6$ configuration of Eu^{3+} ions , among which the main emission line is located at around 611 nm, corresponding to the electric dipole transition of $^5D_0$-$^7F_2$. This emission at 395 nm excitation can be attributed to the sharp lines in the longer wavelength region assigned to the intraconfigurational 4f-4f forbidden transitions of Eu^{3+} that is depicted in figure 3.10 (energy transfer mechanism). Noticeably, the emission brightness is enhanced till 2.5 mol% and after that concentration quenching occurred. With increasing Eu^{3+}concentration, the distance between Eu^{3+} ions decreased and thus the probability of energy transfer was higher. The probability increased with Eu^{3+}concentration. This made it

possible that higher Eu^{3+}concentration lowered the emission energy for transfer from the low ^5D excited state to the ^7F ground state.

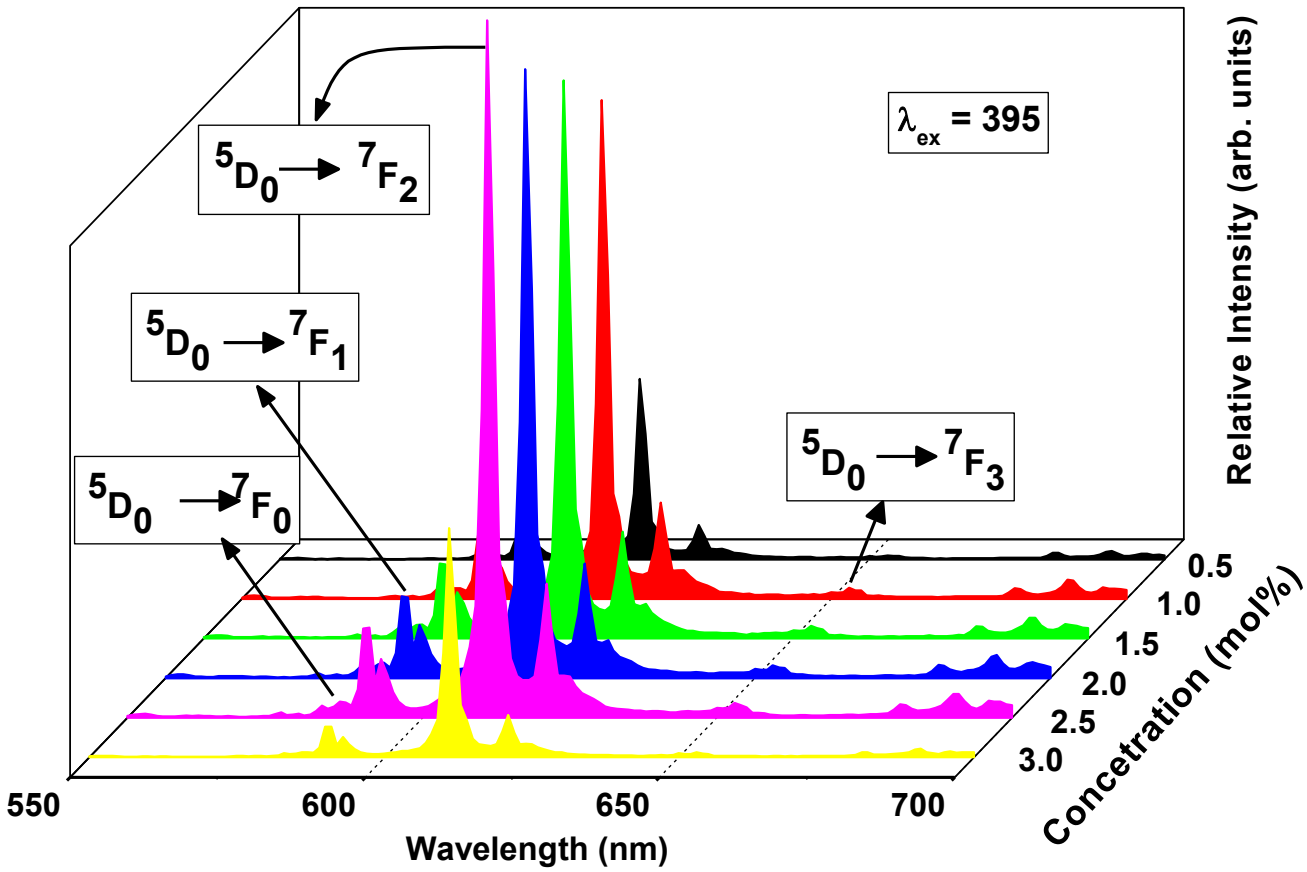

Figure 3.9: Emission spectra of $Ca_{0.9-x}Zn_{0.1}Nb_2O_6$: Eu_x phosphors at 395 nm excitation

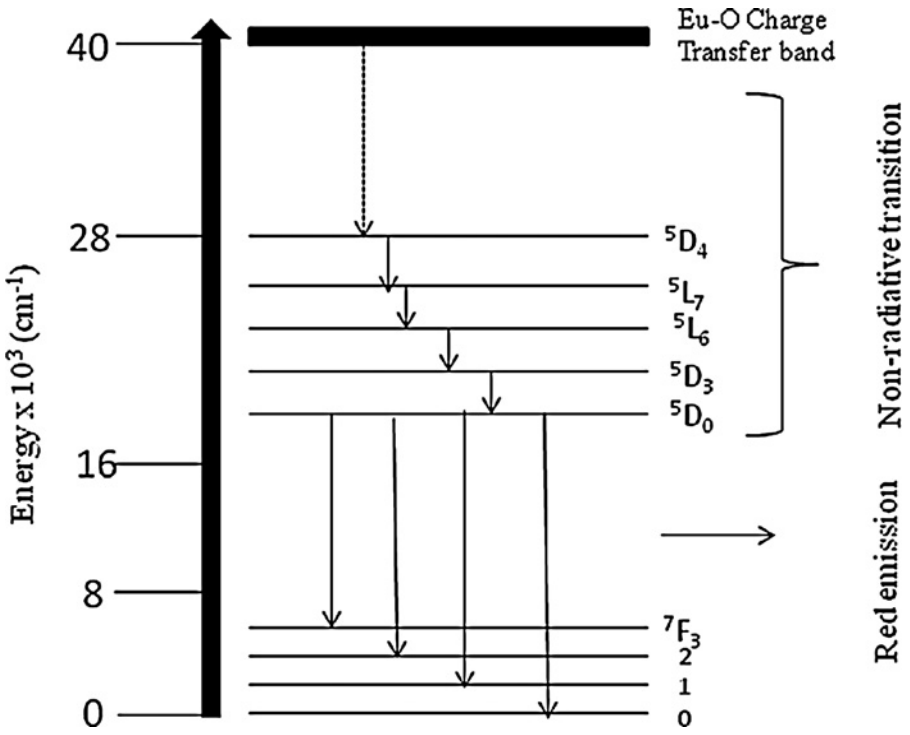

Fig. 3.10: The energy level diagram of Eu^{3+} ion showing the states involved in the luminescence process and the transition probabilities under 395 nm excitation.

3.6 Chromaticity coordinates

The commission Internatinale d'Eclairage(CIE) chromaticity coordinates calculated for $Ca_{0.9-x}Zn_{0.1}Nb_2O_6$: Eu_x phosphors were calculated and indicated in figures 3.11 and 3.12. The emission color analysed with the help of CIE Coordinates. With increasing Eu^{3+} concentration, the CIE coordinates changing from one region to other region due to the energy transfer mechanism mentioned in section 1.4. All these coordinates nearly falling in the CIE white domain only under 266 nm excitation as shown in the figure 3.11. Hence, it can be stated that this phosphor emit white emission under the UV excitation, which will be useful for white light emitting diodes.

In the case of 395 nm excitation, the calculated CIE chromaticity coordinates are found to be (0.64, 0.34) as indicated in figure 3.12, which is close to the standard red chromaticity (0.67, 0.33) for the National Television Standard Committee(NTSC) system. The advantage of this phosphor is that this material can be used in n-UV based RGB white LEDs

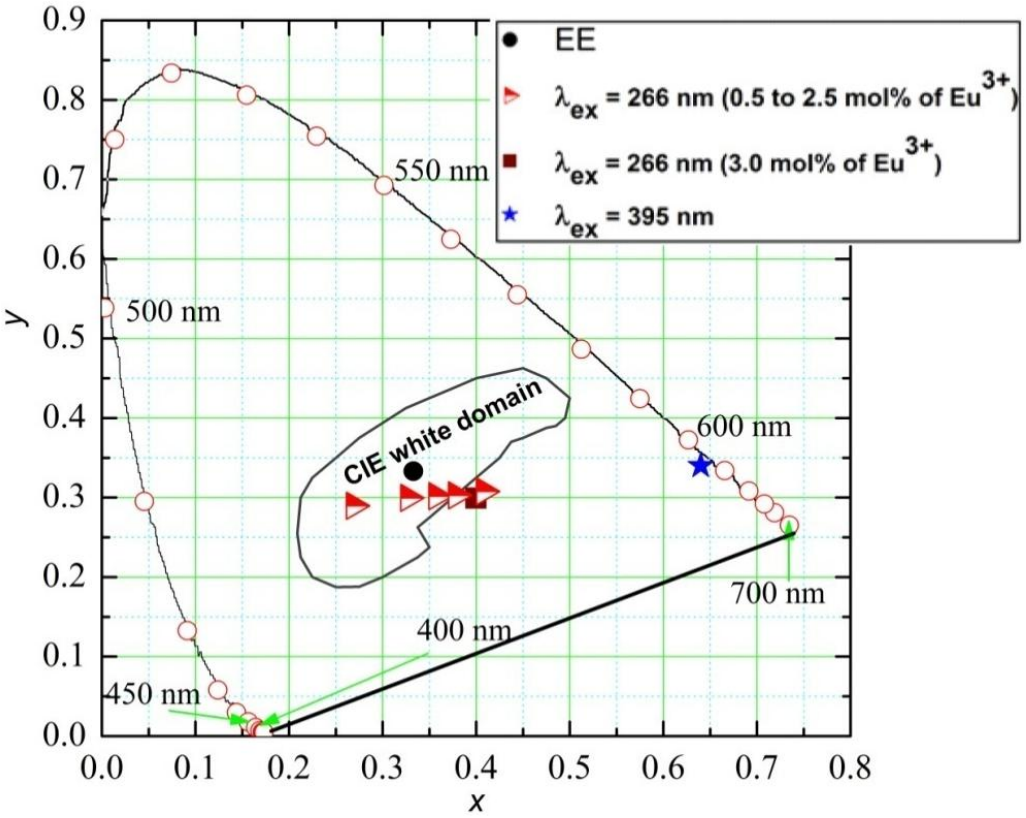

Figure 3.11: Chromaticity coordinates under 266 nm and 395 nm for $Ca_{0.9-x}Zn_{0.1}Nb_2O_6$: Eu_x phosphors

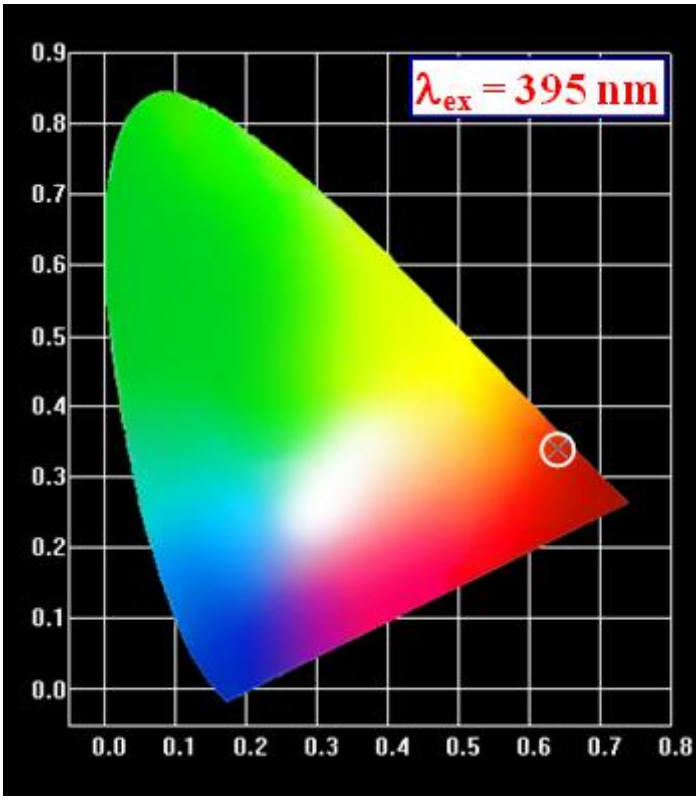

Figure 3.12: Reddish orange emission of $Ca_{0.9-x}Zn_{0.1}Nb_2O_6$: Eu_x phosphors under 395 nm excitation

Conclusions:

Eu^{3+} doped $CaZnNb_2O_6$ phosphors were succesfully synthesized by using conventional solid state reaction method. SEM analysis indicate that these phosphor powder particles are agglomerated and vary from sub-micrometers to micrometers. The excitation spectra indicate that this phosphor could be effectively excited by 266 and 395 nm. The luminescent properties were carried out for different Eu^{3+} concentrations to know the optimised doping concentration and found to be 2.5 mol% of Eu^{3+}. Upon excitation with 266, the phosphor shows one broad band emission at 475 nm related to the pure sample and the 4f-4f emission lines of Eu^{3+}. The CIE chromaticity coordinates results show that these phosphor samples emit white light under 266 nm excitation, which will be useful for UV-based white light emitting diodes. In the case of 394 nm, the samples exhibited only 4f-4f emission lines of Eu^{3+} and emit reddish orange color with chromaticity coordinates (0.64,0.34) close to NTSC standards. Hence, Eu^{3+} doped $CaZnNb_2O_6$ phosphor is a potential candidate for the solid state lighting applications.

References

1. Nag A, Kutty T R N.. Journal of Materials Chemistry, 2004, 14(10): 1598.
2. He H, Fu R, Song X, Wang D, Chen J. Journal of Luminescence, 2008, 128(3): 489.
3. Park J K, Choi K J, Kim K N, Kim C H Applied Physics Letters, 2005, 87(3):031108.
4. Yang J, Quan Z, Kong D, Liu X, Lin J. Growth And Design,2007,7(4):730.
5. Tauc.J,Amorphous and liquid semiconductors,J.Tauc Edi,New York,Plenum,(1974)
6. Hsu C, Powell RC. J.Lumin, 1975, 10(5):273.
7. Li C X, Quan Z W, Yang J, Yang P P, Lin J. Inorg. Chem., 2007, 46(16):6329.
8. Blasse G, Grabmaier B C. Luminescent Materials. New York: Springer-Verlag, 1994.
9. Zhou.Y, Qiu.Z, Lü.M, Ma.Q, Zhang.A, Zhou.G, Zhang.H, Yang.Z, J. Phys. Chem.C 111 (2007) 10190.
10. Hara K, Tominaga S, Takano A, Dantani K, Yoshino J, Kukimoto H, Jpn. J. Appl.Phys. 31 (1992) L1661.
11. Fang T H, Hsiao Y J, Chang Y S, Chang Y H, Mater. Chem. Phys. 100 (2006)418.